GREEN SYNTHESIS OF TITANIUM DIOXIDE NANOPARTICLES USING *DELONIX REGIA* LEAF EXTRACT FOR THE PHOTOCATALYTIC DEGRADATION OF METHYL RED DYE

BY

AYENAJEH, Godwin
MEng/SIPET/2018/8088

A THESIS SUBMITTED TO THE POSTGRADUATE SCHOOL, FEDERAL UNIVERSITY OF TECHNOLOGY, MINNA, NIGERIA IN PARTIAL FULFILMENT OF THE REQUIREMENTS FOR THE AWARD OF MASTER OF ENGINEERING DEGREE IN CHEMICAL ENGINEERING

OCTOBER 2023

ABSTRACT

This research work has demonstrated the viable application of Titanium dioxide nanoparticles in the heterogenous photocatalytic degradation of methyl red dye solution through the Advanced Oxidation Processes (AOPs). The AOPs have demonstrated enormous efficiency in the degradation of both inorganic and organic water pollutants. This work describes the comparison of the sol gel and green synthesis method of Titanium dioxide Nanoparticles (TiO_2 NPs) from Titanium (IV) Butoxide precursor. The sol gel synthesis method has been described to be simple and cost effective whereas the green synthesis approach is eco-friendly, cost effective and efficient. The phytochemicals for the green synthesis route were obtained from *Delonix regia* leaf extract and the phytochemical content of the leaf extract was determined to be total flavonoids (64.76 mg/100 g), total phenols (248.98 mg/100 g), alkaloids (29.56 mg/100g), tannins (107.76 mg/100 g) and saponins (78.97 mg/100g). These phytochemicals acted as the reducing and capping/stabilizing agents in the synthesis of the TiO_2 NPs. The formation of nanoparticles was confirmed via UV-Visible spectroscopy at 376 nm and 364 nm for the sol gel and green catalyst respectively. Booth catalysts were calcined at 300^oC, 350^oC, 400^oC and 450^oC. Over 93 % of methyl red dye molecules were degraded by the TiO_2 NPs calcined at 350^oC and hence considered the most appropriate calcination temperature for the synthesized TiO_2 NPs in the study. The TiO_2 NPs were characterized by Brunauer Emmet Teller (BET), Scanning Electron Microscopy/Energy Dispersion X-ray (SEM/EDX), Fourier Transform Infrared (FTIR) and Xray Diffraction (XRD). Batch photocatalytic experiments showed that the synthesized catalysts via sol gel and the green method degraded methyl red by 92.5% and 93.02% respectively under solar irradiation. Both catalysts prepared in this study performed best in the acidic medium and the experimental data was best fitted into the Pseudo-First-Order kinetics with the regression correlation in the range 64.36 %-83.53% for the green TiO_2 NPs whereas that of the sol gel is in the range 83.03%-95.27% for all concentrations considered in the study.

TABLE OF CONTENTS

LIST OF FIGURES

LIST OF TABLES

LIST OF PLATES

CHAPTER ONE

1.0 INTRODUCTION

1.1 Background to the Study

Many industries especially the textile industry consume great quantity of water in processes such as dyeing and finishing stages. This generates a lot of wastewaters containing colours(dyes) and other chemicals (comprising of between 15-20%). In the event of discharged of such wastewater without prior treatment, it constitutes environmental pollution (land and water) and may as well cause extreme negative effects on health (Akpan and Hameed, 2009).

Several research works have reported numerous physicochemical treatment techniques of Textile Wastewaters (TWW). The common techniques are ultrafiltration, flocculation, activated carbon adsorption, chemical oxidation, biosorption, dye decolouration, membrane filtration, and reverse osmosis (Ashraf, 2021; Akpan and Hameed, 2009). Unfortunately, physicochemical wastewater remediation processes have limitations in applications and disadvantages such high costs and energy requirements, and the creates secondary pollution of environmental concern (Akpan and Hameed, 2009).

In order to mitigate the challenges associated with the physicochemical treatment techniques, recent research works are now been centred on Advanced Oxidation Processes (AOPs). They include the Fenton based process, heterogeneous

photocatalysis, Ultra-Violet based, and Hydrogen peroxide. AOPs are capable to transform completely, organic chemicals like dye into non-harmful products (Pirila *et al*., 2015).

Heterogeneous photocatalysis utilizes photocatalysts like Titanium dioxide (TiO_2), Zinc oxide (ZnO) and Iron oxide (FeO). The photocatalysts display immense ability to destroy pollutions, while evading to create a secondary pollution (Akpan and Hameed, 2011).

Titanium dioxide nanoparticles (TiO_2 NPs) is a unique photocatalyst and mostly easily obtainable, relatively cheap, non-toxic and chemically stable and an excellent photocatalytic ability. Other properties are its high refractive index, high photoelectric conversion proficiency, high dielectric constant, and biocompatibility (Srinivasan, *et al.*, 2019).

The conventional method of synthesizing NPs often involves the use of hazardous chemicals and high energy processes which has made researchers resort to ecofriendly alternatives that utilize natural resources (Ying *et al.*, 2022).

However, these synthesis methods of the TiO_2 NPs have several setbacks, such as environmental toxicity which is first concern, and therefore place a limitation in their application in areas like biotechnology, medicals and pharmacology (Saranya *et al.*, 2018).

Hence, the biosynthesis (green) technique, has become an alternate approach in the synthesis metal oxide NPs since they offer the advantage of eliminating the production of harmful toxic by-products. It is also eco-friendly and time efficient. This has motivated study ways to synthesis and modify metal oxide nanoparticles such as TiO_2 NPs (Aravind *et al.*, 2021).

The green synthesis approach employs metabolites of plants, bacteria and enzymes but plant leaf extract offers high Concentration of phytochemicals/biomolecules such as flavonoids, amino acids, phenols, polysaccharides, tannins and saponins. The phytochemicals reduce and stabilize the NPs during the biosynthesis processes (Zeebaree *et al*, 2022).

Delonix regia, generally called the Flamboyant tree, is a noticeable wild growing and perennial tree. It is flowering a tree common in parks, gardens, along roads and the matured specie provides excellent Shade. It may be useful for herbal application.

The undertaken study compares the Sol-Gel synthesis technique and green synthesis method of TiO_2 nanoparticles. Also, the study verifies the efficiency of the prepared NPs through photocatalytic degradation of an industrial organic wastewater.

The concentration of plant metabolites/phytochemicals plays a vital role in the green synthesis of TiO_2 NPs, either directly influencing yield and most importantly improving the photocatalytic activity (Dobrucka, 2017). Therefore, *Helianthus annus*, commonly known as sunflower plant, was also screened and the phytochemical content compared with that of *Delonix regia* plant.

Methyl red is a common dye used in the textile industry, cosmetics as well as food industry. Its release into the environment poses a significant challenge dues to its potential toxicity and persistence. Photocatalytic degradation of methyl red dye with TIO_2 NPs offers a sustainable solution for its removal, as the NPs are capable of harnessing solar energy to generate reactive species, leading to the mineralization the dye molecules into water and carbon dioxide.

1.2 Statement of the Research Problem

Industrial liquid effluents contain organic pollutants like dye, pesticide, surfactant and chloro-organics which are a serious challenge of the modern-day human population as a result of toxicity, carcinogenic and hazardous effects (Akpan and Hameed, 2009). Conventional treatment techniques have been utilized to remove pollution from effluent streams, however, such techniques are considered ineffective in the destruction of such pollutants and may transfer them unto other medium and creates secondary pollution (Ameta *et al.,* 2013).

The heterogenous photocatalysis with TiO_2 NPs are considered a better approach in the treatment of organic pollutants but the synthesis techniques employ toxic substances resulting from the use of toxic chemicals for the physical or chemical synthesis methods of TiO_2 nanoparticles has been identified as the major challenge which further contribute to environmental pollutions and as well making their applications in the pharmaceutical and medical industry unlikely (Saranya *et al.,* 2018). Other disadvantages of the physicochemical synthesis techniques include expensive cost of chemicals and energy requirements, difficulty in post-production separation and they as well as hazardous nature of the process.

Hence, the biosynthesis (green) technique, has become an alternate approach in the synthesis metal oxide NPs since they offer the advantage of eliminating the production of harmful toxic by-products. It is also eco-friendly and time efficient. This has motivated study ways to synthesis and modify metal oxide nanoparticles such as TiO_2 NPs (Aravind *et al.,* 2021).

1.3 Justification of the Study

This study compared two methods for synthesizing TiO_2 NPs namely; the Sol-gel and green synthesis techniques. The Sol-gel method is relatively cost effective and simple and can be performed under atmospheric conditions.

Whereas the green synthesis method is cost effectiveness and non-toxic in nature several research reports has suggested the viability of this method as a suitable alternative to the orthodox physicochemical techniques.

Plant leaf extract such as *Delonix regia* extract, which contains potential phytochemicals useful in the reduction, and stabilization of nanoparticles, are considered as suitable alternatives to the chemicals usually employed in the synthesis TiO_2 NPs. The use of the plants leaves is also eco-friendly and economical since it does not compete with food, hence, it is sustainable and promotes a cleaner and greener future.

Aim and Objectives of the Study

The aim of the study is to investigate the ability of *Delonix Regia* leaf extract in the synthesis of TiO_2 NPs and to confirm the effectiveness in the degradation of methyl red dye.

It was achieved through the following objectives;

i. Extraction of the *Delonix Regia and Helianthus annus* leaf
ii. Testing and determination of the phytochemical properties/constituent of the plant extract
iii. Synthesis of the TiO_2 NPs through the Sol-gel and green method
iv. Photocatalytic activity test of the produced TiO_2 through degradation of Methyl Red dye (photocatalytic degradation)

v. Characterization of the produced TiO_2 NPs through UV-Vis spectroscopy. FTIR, SEM/EDX, XRD, and BET

vi. Study of the effect of degradation process parameters and kinetics through visible light irradiation.

CHAPTER TWO

2.0 LITERATURE REVIEW

This chapter explains the theoretical background/review of this research work, covering topics such as dyes in textile wastewater, wastewater treatment technologies, titanium dioxide nanoparticles synthesis and application in wastewater remediation.

2.1 Dyes and Textile Wastewater (TWW)

The importance of the textile industry to mankind cannot be overemphasised, unfortunately it is regarded as one of the largest contributors to environmental pollution (Akpan and Hameed, 2009). Due to the nature of processes involved, this industry consumes large volume of water, producing effluents that require high cost of treatment procedures prior to their discharge (Chequer *et al.*, 2013).

The major composition as stated in Lellis *et al.*, (2019) are not limited to the biological oxygen demand (BOD), the chemical oxygen demand (COD), and the non-biodegradable organic dyes but also salinity, pH, and mostly coloration (Chequer *et al.*, 2013).

The textile industrial wastewater (TWW) is also known to contain lots of organic matter which is hazardous to both and the environment. One of the major organic pollutants of concern present in TWW are dyes, chiefly due to their difficulty to degrade during the primary treatment processes (Yaseen and Scholz, 2019).

Dyes are substances that are applied to a substrate to provide colours. This process alters, at least momentarily, any crystal structure of the coloured substances (Chequer *et al.,* 2013). They could be cationic in nature (methylene blue, rhodamine blue, rhodamine 6G, and crystal violet) or anionic in nature (Acid red, methyl orange, Methyl red, acid orange and phenol red) (Rafiq *et al.,* 2021).

It is reported that about 15% of dyes end up in the effluent stream during the dyeing processes and the presence of dyes in water alters its pH, increase both the biological and oxygen demand (BOD and COD) of the receiving water bodies (Rafiq *et al.,* 2021).

The major challenge with dyes is their complicated constituents and high chemical stability, which makes them persist in water and wastewaters, reduce photosynthetic activity, also affects the growth of aquatic living organism by obstructive access to sunlight and cause biological oxygen demand (BOD) and also decrease the recreational worth of a water body (Amini and Ashrafi, 2016).

2.7 Methyl Red Dye

Methyl red dye is a common synthetic dye used as an indicator in laboratory experiments and in the textile dyeing process. It is an azo dye which, generally known to be mutagenic and poisonous when leased untreated along with water into the environment. They are the largest group of synthetic Dyes in the industries, with annually production estimated at 800,000 tons worldwide. These dyes are characterized by double Nitrogen bond (-N=N-). The hydrocarbon rings are characteristically aryl groups which are derived from aromatics. The chemical nature of these dyes renders them very resistant to biological and chemical treatment technologies (Olukani *et al.,* 2019).

The International Union of Pure and Applied Chemistry (IUPAC) standadard numenclature of methyl red dye is 2-(N,N-dimethyl-4-aminophenyl) azobenzenecarboxylic acid ($C_{15}H_{15}N_3O_2$), the chemical structure is on Figure 2.1. Its also known as C.1 Acid red 2. Its characterized colour is dark red crystalline powder at room temperature.

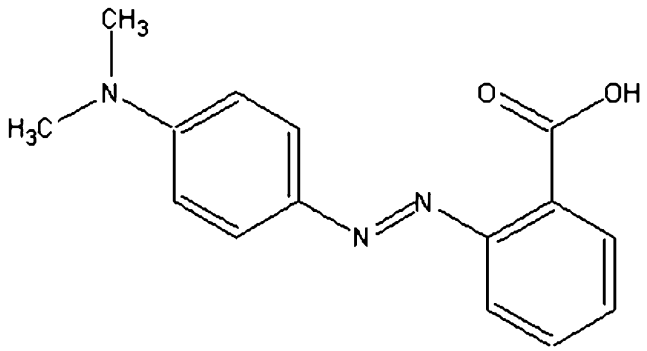

Figure 2.1: Chemical structure of Methyl red (Ashraf *et al.*, 2006)

The common adverse effect of methyl red dye if contacted by humans is eye irritation and skin sensitization. It even causes digestive tract irritation if ingested (Vinoda *et al.*, 2015).

2.8 Processes of Removing Dyes from TWW

Dyes, either the reactive, direct, basic and acid dyes are highly soluble in water. Treatment processes based on Physical (adsorption, Reverse Osmosis, ion exchange, ultrafiltration), Chemical (chlorination and ozonation), Biological (aerobic and anaerobic treatments) and even a combination of the aforementioned can be used to treat TWW (Abdellah *et al.*, 2018).

However, most dyes are difficult to remove via the conventional methods (Lellis *et al.*, 2019) as they are designed to be resistant to biodegradation in order to ensure a larger

lifespan of such a dye (Chequer *et al.,* 2013). Hence, the pollutants may just be transferred, resulting in the creation of secondary pollutants (Akpan and Hameed, 2011)

2.8.1 Advanced oxidation process (AOP)

Advanced oxidation process (AOPs) is a novel pollution treatment technology whose principle and mechanism involves the generation of strong hydroxyl or sulphate radicals through ozone or ultraviolet (UV) irradiation for the oxidation of organic radicals in water.

The Hydroxyl radicals (*OH) can be generated from reactions involving; (a) ozone (O_3), (b) hydrogen peroxide (H_2O_2)—oxidants with high degrading ability, (c) semiconductors such as titanium dioxide (TiO_2) and (d) ultraviolet irradiation (UV) (Bento and Pillis, 2018).

These AOPs has enabled researchers and the industries to bridge the gap of the conventional water treatment processes and as well aid compliance with the stringent environmental sanctions and regulations (Ghime and Gosh, 2020).

2.8.2 Fenton process

This is one of the most efficient AOPs used in the treatment of wastewater. It usually involves the use of H_2O_2 and Fe^{2+} to generate reactive oxygen species in aqueous phase for the degradation of organic and inorganic pollutants. The reaction of H_2O_2 and Fe^{2+} generates a strong reactive specie, *OH, a very active oxidant.

This wastewater treatment process is relatively cheap and easy to handle as both chemicals used are affordable and easily decomposes in the reaction process, making them safe in application.

Equations 2.1-2.7 illustrates the reaction steps involved in the Fenton process:

$$Fe^{2+} + H_2O_2 \rightarrow Fe^{3+} + OH^- + *OH \quad (2.1)$$

$$Fe^{3+} + H_2O_2 \rightarrow Fe^{2+} + HO_2* + H^+ \quad (2.2)$$

$$*OH + H_2O_2 \rightarrow HO_2* + H_2O \quad (2.3)$$

$$*OH + Fe^{2+} \rightarrow Fe^{3+} + OH^- \quad (2.4)$$

$$Fe3^+ + HO_2* \rightarrow Fe^{2+} + O_2H^+ \quad (2.5)$$

$$Fe^{2+} + HO*_2 + H^+ \rightarrow Fe^{3+} + H_2O_2 \quad (2.6)$$

$$HO_2* + HO_2* \rightarrow H_2O_2 + O_2 \quad (2.7)$$

(Mishra *et al.*, 2017)

2.8.3 Heterogeneous photocatalysis

Heterogeneous photocatalysis is a reduction-oxidation reaction initiated by photon energy, in the presence of a catalysts. An effective photocatalytic reaction is possible with nanosized semiconductors. In the photocatalytic process, a semiconductor, for example TiO_2, is excited by photon irradiation whose energy must be same as or above the band gap energy of the photocatalyst and is capable of causing valence electrons transfer to the conduction band and results in the formation of electron–hole pairs (Pirila *et al.*, 2015)

In photocatalysis, anatase TiO_2 NPs provide excellent photocatalytic properties with a bandgap of about 3.1 eV, they absorb the ultraviolet (UV) region of sunlight that leads to electron–hole creation and separation. These charges provide strong oxidizing power allowing organic molecule decomposition (Akpan, 2011).

The term photocatalysis as defined by several authors emphasizes on the importance of light(photon) in the initiation and activation of numerous reactions that mimics photosynthesis. Photocatalysis refers to light assisted reactions which ordinarily are thermodynamically uphill, such reactions are un-spontaneous nature, hence a catalyst is required for the initiation of the process (Zhu and Wang, 2017).

Colmonares and Luque (2014) in their work on heterogeneous photocatalysis stated that in this process, solar photons initiate the reduction-oxidation reactions to produce chemicals (for example, fuels solar photons are used to drive redox reactions to produce chemicals).

Just as in the case of classical catalysis which involves a sequence of five stages, vis-à-vis;

I. Transfer of reactants from the liquid phase to the catalyst surface
II. The adsorption of one of the reactants in the medium
III. A reaction in the adsorbed phase/surface
IV. Desorption of the products of the reaction
V. Transfer of products away from the diphasic area reactions

(Philippoulos and Nikolaki, 2010).

Likewise, Photocatalysis involves the following sequence of processes:

I. The absorption of photon energy to generate electron-hole pairs

II. Excited electron-holes pairs separation

III. The transferring of electrons-holes to the photocatalysts surface

IV. Sometimes, the recombination of electrons-holes

V. Application of charges on the surface for reduction and oxidation reactions

As in the case of catalysis whose reaction involves the use of catalysts to initiate a reaction, whereby itself remains unchanged at the end of the reaction. Photocatalytic reactions on the other hand, are thermodynamically uphill reactions that are photon induced (Zhu and Wang, 2017). The equations of photocatalytic reaction are described in equations 2.8-2.11:

1 Photon activation of TiO_2

$$TiO_2 + hv \rightarrow e^- + h^+ \quad (2.8)$$

2 Oxygen adsorption

$$O_2 + e^- \rightarrow O_2^{*} \quad (2.9)$$

3 Water ionization

$$H_2O \rightarrow OH^- + H^+ \quad (2.10)$$

4 Superoxide protonation

$$O_2^{*} + H^+ \rightarrow HOO^{*} \quad (2.11)$$

(Colmonares and Luque, 2014)

The photocatalytic process is schematically described in Figure 2.1. it shows how photon energy from a light source, the sun, excites electrons from the valence band to the conduction band of a semiconductor. Thus, enabling adsorption and reduction of

oxygen (O^{2-}) ions on one hand the oxidation and adsorption of water (H_2O) and pollutants on the other hand.

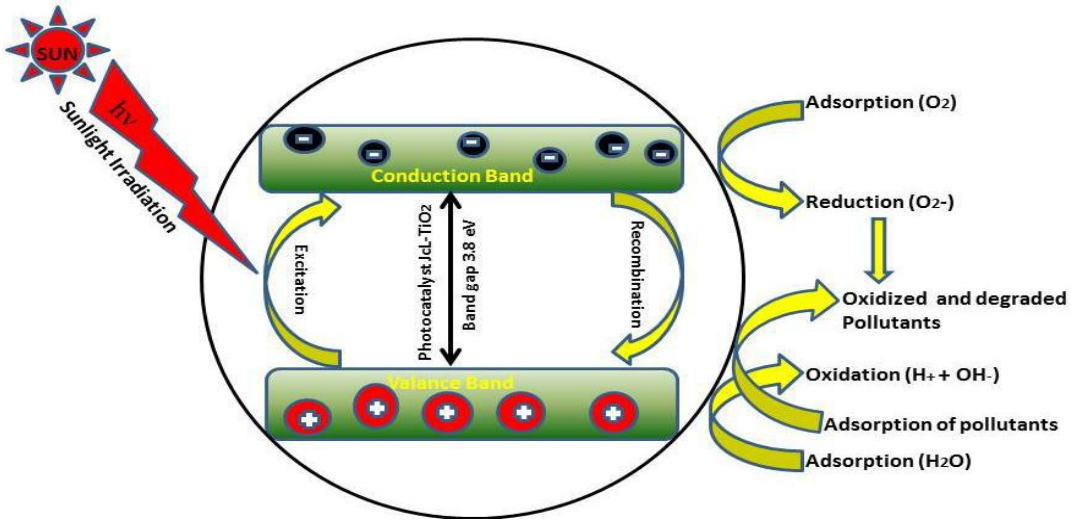

Figure 2.2: Schematic representation of heterogeneous photocatalytic process (Goutam *et al.*, 2017)

Hence, a very good photocatalyst is capable of converting solar energy into chemical energy. Thus, it is important both for environmental (water treatment, air purification, self-cleaning surfaces) and energy (Hydrogen H_2, production by water cleavage and carbon dioxide CO_2, conversion to hydrocarbon fuels) applications (Moma and Baloyi, 2018).

2.9 Titanium Dioxide NPs in Heterogeneous Photocatalysis

Among the diverse NPs in application, TiO_2 NPs has attracted high consideration and has been synthesized or both small- and large-scale applications (Nadeem *et al.*, 2018). The use of TiO_2 photocatalysis is attributed to it is largely availability, low-cost, and non-toxic and relatively stable-chemically. Its other characteristics are high refractive index, high dielectric constant, high photoelectric conversion efficiency, and

biocompatibility (Riaz *et al.,* 2013); it is also insoluble in water and highly resistant to chemical attack (Abhang *et al.,* 2011). This compound exists in three (3) forms (Figure 2.2) namely; anatase, rutile, brookite. The Anatase phase is crystalline and looks like tetragonal system (with di-pyramidal habit) and is mostly applied as a photocatalyst. The Rutile type TiO_2 also has a tetragonal crystal structure (Amanulla and Sundaram, 2019) Anatase TiO_2 is the most preferred in application due to its increased photocatalytic activity (Macwan *et al.,* 2011).

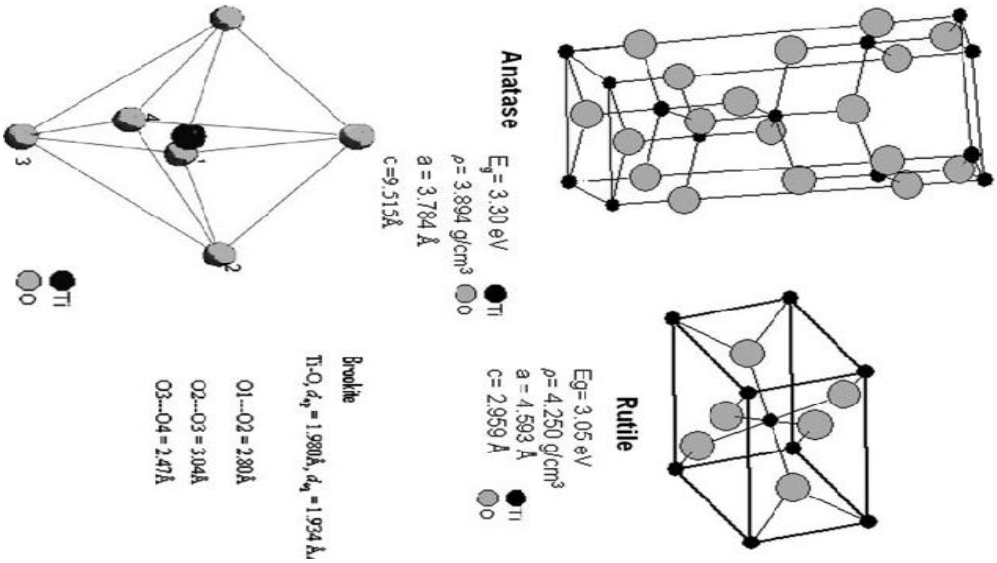

Figure 2.3: The three forms/phases of TiO_2 (Nyamukamba *et al.,* 2018)

TiO_2 NPs use in heterogeneous photocatalysis wastewater treatment process is highly due to the ease in application at room temperature. Also, the process is able to completely mineralise the pollutants into Carbon dioxide (CO_2) and Water (H_2O) and Hydrochloric acid (HCl), without producing intermediates. The catalyst can as well be easily supported on various materials such as Activated carbon, fibres, glass and stainless steel, making its reusability highly feasible (Akpan and Hameed, 2009).

The following are some common commercial nanoparticles; ST-01 and ST-20 from Ishihara Sangyo, Hombikat 100 from SachtlebenChemie and P25, and P90 from EvonikDegussa (Balkus, 2013).

2.10 Conventional Synthesis of TiO_2 NPs

Many research works have reported the synthesis of TiO_2 NPs and their successful applications. The physicochemical synthesis routes offer a range of advantages such ease and large-scale production among others.

The various physicochemical synthetic processes are the chemical and physical (CVD and PVD) deposition, hydro/solvothermal, oxidation, sonochemical and microwave assisted methods and the sol-gel method among others.

The sol-gel synthesis of TiO_2 NPs is the conversion of a precursor solution (usually a metal alkoxide) into an inorganic solid via a polymerization reaction induced by water. The process involves hydrolysis (forming a sol) and condensation (forming the gel). The many advantages of this technique include low operating temperature, homogeneity of molecules and the ease of control of the particle sizes and manipulation of gel into desired shapes (Nyamukamba *et al.,* 2018).

Some of the advantages and disadvantages of the conventional synthesis techniques (bottom-up methods) of titanium dioxide nanoparticles are highlighted on Table 2.1.

Table 2.1: Advantage and disadvantage of conventional synthesis techniques of TiO_2 NPs

Advantage	Disadvantage
Allows the ease of control of particles size and morphology	Complex processes and requires specialized equipment which contributes to the high production cost
Enhance high purity of products for specialized applications such as in electronic devices	Involves multi-step processes such as nucleation, growth and post treatment, this results in longer processing time
Product homogeneity with uniform composition and distribution	Poses a scale-up challenge in areas particle size and morphology control, where large product volume is a criterion
Properties of the nanoparticles can be easily tailored for customized applications by modifying synthesis parameters	Techniques are usually sensitive to reaction conditions such as pH, temperature and pressure

(Nyamukamba *et al.*, 2018)

2.11 Green Synthesis of TiO_2 NPs

Green synthesis method of TiO_2 NPs involves usage of eco-friendly, biodegradable and non-toxic substances as the reducing and stabilizing agents. Several natural sources such as plants, algae, fungi, bacteria and even waste materials have been exploited in the green synthesis of TiO_2 NPs.

These green methods of synthesizing NPs offer variable merits such the availability of precursor materials, cost effectiveness, environmental friendliness and safety and it also presents a broad viability of metabolites (Abisharan, *et al.*, 2019).

Major literature has reported the use of different biological metabolite sources such plants, microbes and related bio-products, however, plant species has been considered the most suitable (Nadeem *et al*., 2018).

The complete green synthesis process is illustrated in Figure 2.3. Simply, a plant or bio-extract is added to a titanium precursor and mixed thoroughly. The constituents of the extract present reduce- and stabilize- the bulk metal into nanoparticles.

The reaction proceeds at a rapid rate, a change of colour indicates the first sign of NPs formation which can then be confirmed by UV-Visible spectroscopic techniques. Colour change could be greenish or dark green as on the formation of TiO_2 NPs (Rajakumar *et al*., 2012).

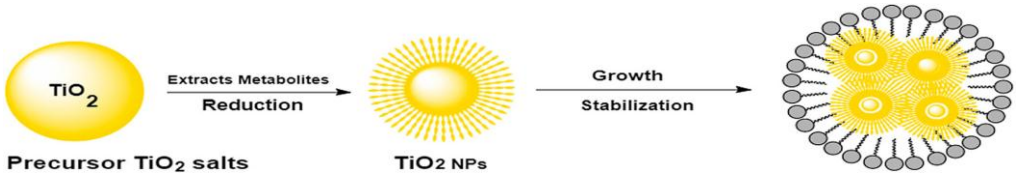

Figure 2.4: Reduction mechanism of TiO_2 NPs (Nadeem *et al*., 2018)

A large part of literature reported on green synthesis studies were conducted using various types of leaf extracts, due to their enrichment in metabolites/phytochemicals. In a study conducted by Roopan *et al.*, (2012), spherical TiO_2 NPs were obtained when *Annona squamosa L*. extract was added to TiO_2 salt solution at room temperature.

The use of *Calotropis gigantea* leaf extract was reported to reduce TiO_2 to NPs in 6 h. The excellent bio-reduction potential was credited to the presence of primary amines in the extract (Marimuthu *et al.,* 2013).

In another report, TiO_2 NPs were synthesized with extract of *Catharanthus roseus L.* The aliphatic alcohols and amine constituents of the extract contributed to synthesis of TiO_2 NPs. Particles with 25–110 nm size and irregular shapes were obtained (Velayutham *et al.,* 2011). *Morinda citrifolia L*. extract has also been reported. The resultant NPs were confirmed through analytical characterization (Sundrarajan *et al.,* 2017).

Also, TiO_2 synthesized using orange peel extract by Amanulla and Sundaran (2019) showed the XRD pattern formation of an anatase phase for nanoparticles with crystallite size of 17.30 nm. SEM analysis of the TiO_2 NPs showed the particles have highly porous angular morphology, FTIR confirmed the presence of carbohydrates and fatty acids in the orange peel extract.

TiO_2 NPs has been synthesized using extracts of *Echinacea purpurea* herb a with particle size of 120 nm, an intense signal at 4.5 KeV strongly suggests the presence of titanium nanoparticles (Dobrucka, 2015). Abisharan *et al*., (2019) synthesized TiO_2 NPs using Cucurbita pepo seeds extract, XRD result shows that the particles were tetragonal structure.

The merits and demerits of the green method for the synthesis of TiO_2NPs are briefly highlighted on Table 2.2.

Table 2.2: Advantage and disadvantage of the green synthesis techniques of TiO_2 NPs

Advantage	Disadvantage
Environmentally friendly and minimizes the use of hazardous chemicals, and encourages use of renewable and biobased resources	May not be easily scaled up for industrial production of nanoparticles
Products are biocompatible and suitable for medical and pharmaceutical applications	Suffers some limitations in the particle size and morphology control of products
Minimizes energy consumption, generates less waste and by-products	Complex optimization of reaction parameters to achieve desired products

(Chauhan *et al.,* 2012; Nadeem *et al.,* 2018)

2.12 Applications of TiO_2 NPs

There are several areas that TiO_2 NPs has found significant applications over the years. Such areas include but not limited; photocatalysis and solar cells, Biomedical and healthcare products, environmental remediation, energy storage and conversion, and self-cleaning surfaces (Abbasi, 2021).

A detailed principle of photocatalysis have been explained in section 2.3.3.

2.13 Experimental Study of Photocatalytic Reaction Parameters

The following photocatalytic variables plays important factor during degradation of organic dyes in wastewater are catalyst dosage, solution pH, initial dye concentration, calcination temperature, irradiation time, oxidizing agents and light intensity (Bento and Pillis, 2018).

The first three listed above have been studied in the course of this research due to their immense influence in the degradation of methyl red dye in solution.

2.13.1 Catalyst dosage/loading

The catalyst dosage plays a vital role in the photocatalytic degradation of organic pollutants either in gaseous or aqueous state. As reported by Umar and Aziz (2013), at the onset of an experiment, the amount of catalyst is directly proportional to the photocatalytic reaction rate. On continuous increase in the catalyst dosage, a saturation point is reached, and a decrease in photon adsorption co-efficient occurs, and the excess photocatalyst creates a photon shielding effect, resulting to the reduction in the surface area exposed to irradiation and thereby reducing the photocatalytic efficiency of the process.

Akpan and Hameed (2009) and Singh and Borthakur (2018), further reiterates that photocatalytic degradation eventually decreases when the catalyst dosage exceeds the optimum, due to the suspension of particles which blocks light rays.

2.13.2 Solution pH

It is highly imperative to study the effect of solution pH since most of the industrial textile effluent may not necessarily be neutral (Rafiq *et al.*, 2021). The pH of wastewater or solution performs a critical and complex part in the photocatalytic process of degrading the wastewater in that the pH of a solution is able to affect the catalyst particles surface charge, and conductance, and this reduces the efficiency of the photocatalytic process (Umar and Aziz, 2013; Singh and Borthakur, 2018). Reza *et al.*, (2017) in their review work stated that the nature of the organic dye determines whether a lower (acidic) or higher (alkaline) pH will affect its adsorption onto the TiO_2

photocatalyst. The possible explanation being that TiO_2 shows an amphoteric character, hence, either a positive or a negative charge can be developed on its surface. Hence, a pH variation can affect the adsorption of the dye molecules onto the TiO_2 surface.

The behaviour of TiO_2 NPs under either acidic or alkaline condition can be expressed by Equations 2.12 and 2.13:

$$TiOH + H^+ \rightarrow TiOH_2^+ \quad (2.12)$$

$$TiOH + {}^-OH \rightarrow TiO_2 + H_2O \quad (2.13)$$

This implies that in acidic condition, the catalyst will be positively charged, behaving like an oxidizer whereas in an alkaline condition, the catalyst will be negatively charged, decreasing the reaction rate (Suresh *et al.,* 2018).

2.13.3 Initial dyes concentration

The initial dye pollutant concentration in the effluent stream affects the rate at which it can be decolourized by a semiconductor. This implies that as the concentration of the pollutant in an effluent stream increase subjected to a specific dose of solid photocatalyst, the degradation efficiency will decrease with time, given that the absorptive sites of the catalyst will become less unavailable (Suresh *et al*.,2018). This implies that a photocatalytic process occurs on the absorptive sites and not in the bulk solution (Rafiq *et al.,* 2021). Hence, when all the available active sites of the catalysts are already occupied, the photon irradiation will only reach the dye pollutant and not the catalyst particles, limiting its degradation efficiency.

2.8.4 Catalyst calcination temperature

Shah and Rather (2021) reported the phase transition of TiO_2 NPs of 300-1000^oC calcination temperatures. Pure anatase phase TiO_2 NPs occurs at 300^oC while pure rutile phase occurs at 1000^oC. However, a mixed anatase and rutile phase occurs at 600^oC. There is also a corresponding increase in crystal particles size as the calcination temperature increases.

Kim *et al.,* (2021), further reiterated that crystallinity, crystallite sizes and particle size of nanoparticles is greatly increased by calcination temperature, however, a high temperature reduces the energy band gap and surface area of the NPs. They reported that at 700^oC, the synthesized NPs exhibited optimum photocatalytic performance.

Hence, it can be deduced that calcination temperature can be manipulated to obtained TiO_2 NPs with improved photocatalytic properties that can greatly increase the degradation potential in dye removal from wastewater.

CHAPTER THREE

3.0 MATERIALS AND METHODS

3.1 Raw Materials, Chemicals and Equipment

The various raw materials, chemicals and equipment that were used in the course of the experimental work in the study are stated in the proceeding sections and tables.

3.1.1 Raw materials

The *Delonix regia* commonly known as Flamboyant tree and *Helianthus annus* commonly known and sunflower, were used in the study. The leaves were locally obtained from the Federal University of Technology, Gidan Kwano campus, Minna, Niger state.

3.1.2 Chemicals and reagents

The chemicals and reagents used to conduct this research are of analytical grade. They were used as received without modification and are presented on Table 3.1

Table 3.1: Chemicals and Reagents

Chemical	Formulae	Source
Titaniu butoxide	$Ti(OBu)_4$	Sigma Aldrich
Ethanol	C_2H_5OH	Chemical Engineering Lab., FUTMinna
Hydrochloric acid	HCl	Chemical Engineering Lab., FUTMinna
Sodium hydroxide	NaOH	Chemical Engineering Lab., FUTMinna
Distilled water	H_2O	Chemical Engineering Lab., FUTMinna
Sulphuric acid	H_2SO_4	Chemical Engineering Lab., FUTMinna

3.1.3 Equipment and their sources

The various equipment that was employed at one stage or the other to synthesis TiO_2 and conduct the photocatalytic experiments are presented in Table 3.2

Table 3.2: List of Equipment

Equipment	Model	Source
SEM	PRO:X 800-07334	Central research Lab, Yar'adua University, Katsina
XRD	ARL'XTRA, SN: 197492086	Central research Lab, Yar'adua University, Katsina
BET	Quantachrome, version 11.03	Central research Lab, Yar'adua University, Katsina
FTIR		University of Ilorin
UV Spectrophotometer	Shimadzu-1800	STEP B Lab, FUTMinna
Oven Dryer	DK-VD0010	STEP B Lab, FUTMinna

3.2 Pre-treatment of the Precursor

Fresh leaves of *Delonix regia* and *Helianthus annus* were washed thoroughly with clean water, and further rinsed with distil water to completely remove dirt. They were shade-dried at room-temperature for 10days until samples were completely moisture free. They were then grinded into a fine powder, then stored for further work.

Plate I: Fresh leaves of *Delonix regia*

Plate II: Powdered leaf of *Delonix regia*

3.2.1 Extraction of plant leaf (*Delonix regia and Helianthus annus)*

Aqueous extraction method used by Dobrucka (2017) was adopted. 1, 3 and 5 g of *Delonix Regia* leaf powder was added into 100 mL distil water and boiled at temperature of 60ºC for 30 min. It was left to cool to room temperature before filtering. The supernatant cold stored for later used for the preparation of TiO_2 NPs.

Plate III: Extraction and Filtration of leaf samples

3.2.2 Determination of the phytochemicals in the extract

Phytochemical test of the *Delonix regia* and *Helianthus annus* leaf extract was conducted to detect the presence of the different chemical compounds such as flavonoids, saponins, phenols, tannins and alkaloids.

3.2.2.1 Determination of saponins

0.5 g of the sample was added to 20 mL of 1 N HCl and was boiled for 4 h. On cooling, it was filtered and 50 mL of petroleum ether was added to the filtrate for ether layer and evaporated to dryness. 5 mL of acetone ethanol was added to the residue. 0.4 mL of each was taken into 3 different test tubes. 6 mL of ferrous sulphate reagent was added into them followed by 2 mL of concentrated H_2SO_4. It was thoroughly mixed after 10 min and the absorbance was taken at 490 nm. Standard saponin was used to establish the calibration curve.

3.2.2.2 Determination of tannins

0.2 g of sample was measured into a 50 mL beaker. 20 mL of 50% methanol was added and covered with para film and placed in a water bath at 77-80^{O}C for 1 h. it was shaken thoroughly to ensure a uniform mixture. The extract was quantitively filtered using a double layered Whatman No.41 filter paper into a 100 mL volumetric flask, 20 mL water added, 2.5 mL Folin-Denis reagent and 10 mL of Na_2CO_3 were added and mixed properly.

The mixture was made up to mark with water mixed well and allowed to stand for 20 min for the development of a bluish-green colour. The absorbance of the tannic acid standard solutions as well as samples were read after colour development on a UV-Spectrophotometer Model 752 at a wavelength of 760 nm.

3.2.2.3 Determination of total phenols

The total phenol content of the crude extracts was determined according to the method reported by Innalegwu *et al,* (2017). A 0.5 mL (1 mg/mL) was oxidized with 2.5 mL of 10% Folin-Ciocalteau's reagent (v/v) and neutralized by 2 mL of 7.5% sodium carbonate. The reaction mixture was incubated for 40 min at 45°C and the absorbance was taken at 765 nm using the double beam Shimadzu UV spectrophotometer, UV-1800. The total phenol content was subsequently calculated using Gallic acid as standard.

3.2.2.4 Determination of alkaloids

A 0.5 g of the crude extract was mixed with 5 mL of 96% ethanol -20% H_2SO_4 in ratio (1:1) and filter. 1 mL of the filtrate was added to 5 mL of 60% H_2SO_4, the mixture was allowed to stand for 5 min and 5 mL of 0.5% of formaldehyde solution was added and allowed to stand for 3 h. The absorbance was taken at a wavelength of 565 nm using

Shimadzu UV spectrophotometer, UV-1800. The concentration of alkaloid in the sample was calculated using the molar extinction coefficient of Vincristine, ε=15136 mol/cm.

3.2.2.5 Determination of total flavonoids

Aluminium chloride colorimetric method reported in Innalegwu *et al.,* (2017) was used for flavonoid determination. A 0.5 mL (1 mg/mL) of the plant crude extract was mixed with 1.5 mL of methanol, 0.1 mL of 10% aluminium chloride, 0.1 mL of 1 M sodium acetate and 2.8 mL of distilled water and kept at room temperature for 30 min. The absorbance of the reaction mixture was taken at 415nm with a double beam Shimadzu UV spectrophotometer, UV-1800. The calibration curve was prepared by using quercetin solutions at concentrations of 12.5 to 100 g/mL in methanol.

3.3 Synthesis of TiO_2 NPs

This research study covers two routes for the preparation of TiO_2 NPs photocatalyst. The first method is Sol-gel synthesis technique, which is a chemical approach while the second method was a green chemistry approach using *Delonix regia* plant extract. Titanium butoxide was the precursor salt used in both cases and detailed procedure is stated thus.

3.3.1 Green synthesis of TiO_2 nanoparticles

The green synthesis process of TiO_2 nanoparticles (NPs) is illustrated in Figure 3.1 and can be described briefly as follows:

A total of 20 mL of *Delonix regia* leaf extract was mixed with 5 mL of titanium butoxide and stirred for 30 minutes. This step ensured the incorporation of the plant extract into the synthesis process. To adjust the pH to an alkaline state, a 1 M solution

of sodium hydroxide was dropwise added to the mixture. The resulting gel was allowed to age for 24 hours, facilitating the formation of a stable gel structure. The aged gel was then dried to remove any remaining moisture. Once dried, it was transformed into a fine powder.

The powder was calcined at various temperatures, specifically 300°C, 350°C, 400°C, and 450°C. Calcination involves heating the material to high temperatures to induce chemical and physical alterations.

By following this process, TiO_2 NPs were successfully synthesized using the green method, incorporating the beneficial components from *Delonix regia* plant extract.

The produced catalysts were stored properly for further characterization and photocatalytic studies.

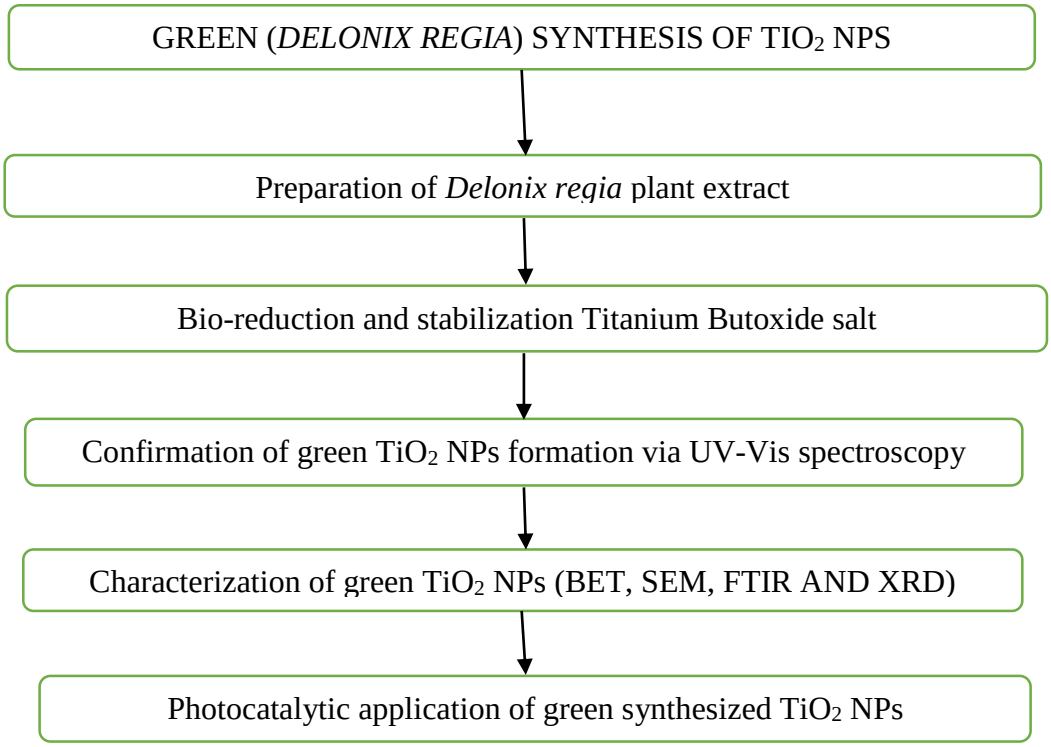

Figure 3.1: Schematic flowchart of green synthesis of TiO_2 NPs

3.3.2 Sol-gel synthesis of TiO_2 NPs

The stepwise procedure for the sol-gel synthesis of TiO_2 NPs highlighted thus (Adopted from Akpan and Hameed, 2011):

i. Solution A: Contains 5 mL of $Ti(OBu)_4$ mixed with 50 mL of ethanol. The solution is constantly stirred using a magnetic stirrer for 1h
ii. Solution B: This contains distil water (H_2O), ethanol (CH_2OH_5) and concentrated nitric acid (HNO_3) with 3:7:1 volume ratio. Solution B is added dropwise into solution A with constant stirring for 3 h
iii. The mixture (gel) is allowed to age for 24 h
iv. The gel was oven dried at 100^oC for 12 h
v. The resultant photo catalyst is then grinded and calcined at 350^oC for 3 h
vi. The catalyst was then stored for characterization and experimental works.

3.3.3 Characterization of TiO_2 NPs

Optical properties were determined using an Ultra Violet (UV)-visible spectrophotometer

(Shimadzu-1800) over the spectral region 200–800 nm. This technique assisted in the confirmation of the formed TiO_2 NPs. The absorbance data was used to determine the energy band gap of the synthesized TiO_2 NPs using the Tauc method based on the assumption that the energy-dependent absorption coefficient α, as expressed by the equation 3.1 and deduced from Tauc plots (Makula *et al.*, 2018).

$$(\alpha - hv)^{1/\gamma} = B(hv - E_g) \quad (3.1)$$

Where h is the Planck's constant, ν is the photon's energy frequency, E_g is the band gap energy and B is a constant. The γ factor depends on the nature of the electron transition and is equal to ½ 0r 2 for the direct or indirect transition band gaps respectively.

The elemental composition and morphology of TiO_2 nanoparticles were determined using a PRO:X 800-07334 Scanning Electron Microscope (SEM) and Energy-dispersive X-ray spectroscopy (EDX) measurements were carried out using a scanning electron microscope equipped with an EDX attachment scanning electron microscope.

Fourier Transform Infrared spectroscopy (FTIR) analysis, a spectrometer with the spectral range set between 4000 and 400 cm^{-1} was used to study the functional groups attached to the TiO_2 NPs and the surface area of the TiO_2 NPs was analyzed using the Brunauer–Emmett–Teller (BET, Quanta chrome, version 11.03) technique.

Lastly, the crystallinity and particle size were analyzed using the Xray Diffraction (XRD, ARL'XTRA, SN: 197492086).

The average particle size was determined by the Scherrer's formula (Equation 3.2)

$$D = \frac{K\lambda}{ß cos\theta} \qquad (3.2)$$

where, D denotes average crystallites size or NPs' mean diameter,

K is Scherrer's constant (0.94)

λ is the X-ray radiation wavelength (0.15406 nm)

β is XRD peak at the diff raction angle θ (rads)

(Irshad *et al.*, 2020)

3.4 Pre-Photocatalytic Experiments

To establish that the dye removal was enhanced by the synthesized TiO_2 NPs catalyst, adsorption and photolysis experiments were first conducted on a Methyl Red dye solution as a simulated model pollutant and the procedures hereby stated as follows. All experiments were conducted at room temperature and atmospheric pressure.

3.4.1 Photolysis

In the photolysis experiment, 100 mL of simulated Methyl Red dye solution was subjected to sunlight irradiation without a catalyst for a period of 3 h. A sample was taken for UV-Spectrophotometric analysis.

3.4.2 Adsorption

0.1 g of prepared TiO_2 NPs was carefully added into the simulated Methyl Red dye solution in a dark medium and continuously stirred for 3 h. A sample was taken for UV Spectrophotometric analysis to ascertain if the degradation is controlled by adsorption.

3.4.3 Photocatalytic degradation of methyl red dye

The synthesized TiO_2 NPs photocatalysts were subjected to activity test using methyl red dye solution as a model pollutant. In all the performed experiments, 0.1 g of each of the synthesized photocatalysts and 100 mL of 45 mg/L dye solution was used. Care was taken to adjust the initial dye concentration to acidic pH with 1 M hydrochloric acid. The mixture was vigorously agitated in a dark medium for 30 min to attain absorption-desorption equilibrium, and then exposed to the sunlight for photon activation of the catalyst and agitated for 3 h. A sample was then withdrawn, centrifuged and analyzed with a UV spectrophotometer to measure the absorbance.

The result of the analyte was changed from absorbance(nm) to concentration (mg/L). The degradation effectiveness of the catalyst was calculated from Equation 3.3:

$$Degradation\ (\%) = \frac{(C_i - C_f)}{C_i} \times 100 \quad (3.3)$$

C_i, initial Concentration,

C_f, final Concentration (Abdellah *et al*, 2018)

3.5 Study of the Degradation Parameters

The influence of photocatalytic degradation variables like dosage, pH of solution, initial concentration and reaction time were studied and described as thus. All the experiments were performed at 25^{o}C and 1 atm.

3.5.1 Effect of catalyst dosage

A catalyst dose of 0.1 to 0.5 g was mixed with 100 mL (45 mg/L) of the dye solution and vigorously agitated in a dark medium for 30min to enable absorption/desorption equilibrium and then exposure to sunlight irradiation for photon activation under constant agitation. Sample solutions were then drawn at regular time intervals of 0, 30, 60, 90, 120, 150, 180 min and centrifuged before analysing with a spectrophotometer to evaluate the absorbance.

3.5.2 Effect of solution pH

The initial pH of the dye was used across a range of values to examine the impact of pH on the degradation process through photocatalysis. The pH levels tested included 2, 3, 4, 8, and 10. Adjustments to pH were made by employing dilute hydrochloric acid and sodium hydroxide solutions. The concentration of the Methyl Red dye solution

remained constant throughout the experiment. Sample solutions were then drawn at regular time intervals of 0, 30, 60, 90, 120, 150, 180 min and centrifuged before analysing with a spectrophotometer to evaluate the absorbance.

3.5.3 Effect of initial dye concentration

The catalyst dosage determined as optimal in section 3.5.1 was employed to examine the influence of dye concentration. Initial concentrations were altered within range of 10-50 mg/L. Similarly. as stated in section 3.5.2, sample solutions were collected at regular intervals of 0, 30, 60, 90, 120, 150, and 180 minutes. These samples were then subjected to centrifugation and analyzed using a spectrophotometer to measure the absorbance.

CHAPTER FOUR

4.0 RESULTS AND DISCUSSION

This chapter highlights the key findings in the undertaken study and the possible inferences that were observed.

4.1 Phytochemical Analysis

Two different plant leaf samples were studied to determine their phytochemical constituents and to analyze which of them will be more viable in the synthesis of TiO_2 NPs. The total phenols, flavonoids, tannins and alkaloids are phytochemicals considered in the reduction and capping of TiO_2 NPs. Their respective constituents in the two plant leaves samples are hence shown on Table 4.1

Table 4.1: Phytochemicals test results of the *Delonix regia* and *Helianthus annus* extract

Sample	Phytochemicals (mg/100 g)				
	Phenols	Flavonoids	Tannins	Saponins	Alkaloids
A	149.38	48.66	53.46	86.95	32.94
	150.89	48.90	54.51	87.44	31.21
B	248.43	63.26	108.37	78.97	28.65
	248.98	64.76	107.76	77.89	29.56

Sample A is *helianthus annus* leaf extract while sample B is the *Delonix regia* leaf extract.

It is paramount to determine the nature of the plant extract, and its concentration because its combine effect with other variables like precursor metal salt concentration, reaction time and the solution pH, affects the rate of production of the NPs and their

resultant characteristics (Dwivedi and Gopal, 2010). Hydroxyl and carboxylic groups present may act as reducing agent and stabilizing agents in the synthesis of nanoparticles (Mohamad *et al.*, 2014)

Delonix regia plant extract contains a more significant amounts of metabolites with an average of 248.7 mg/100 mL total Phenols, 64 mg/100 mL Flavonoids, 108 mg/100 mL Tannins, 78.4 mg/100 mL Sapponins and 29.1 mg/100 mL Alkaloids. These metabolites perform significant role in reducing and stabilizing/capping of TiO_2 NPs and was adopted in the study.

4.2 Study of the Effect of *Delonix regia* Leaf Extract Concentration and Calcination Temperature on TiO_2 NPs

Plant extract concentration perform a significant function in the synthesis of TiO_2 NPs via the green method and its ability to degrade organic pollutants. This was investigated by varying *Delonix regia* leaf concentration during extraction between 1-5 g. Equal volume of 20 mL the leaf extract was used in the green synthesis procedure stated in section 3.3.1.

Table 4.2: Effect of Extract Concentration on TiO_2 NPs Photocatalytic Degradation

Extract concentration g/100mL	% Degradation
B1	92.86
B3	85.08
B5	82.50

Note: B1, B3, and B5 refers to 1, 3, and 5 g of leaf powder

The results as shown in Table 4.2 explains the effect of plant leaf concentration. The prepared catalysts performance was determined in the photocatalytic degradation of methyl red dye solution. It shows that a lower concentration, 1 g/100mL of plant leaf

extract in TiO_2 NPs gave a better photocatalytic performance. This result agrees with the proposal by Mondal *et al.*, (2011) that excess concentration of plant extract will stick to on the surface of the synthesized nanoparticles thereby preventing particle aggregation.

Therefore, considering that the green catalyst prepared with 1 g/100 mL concentration of leaf extract gave a better photocatalytic performance, the catalyst was then calcined at different temperatures, 300^{o}C, 350^{o}C, 400^{o}C and 450^{o}C respectively to examine the influence of calcination temperature. The degradation results are as shown in Figure 4.1a for the green TiO_2 NPs and Figure 4.1b for the Sol-gel TiO_2 NPs. The degradation plots depict that 350^{o}C and 400^{o}C are better calcination temperatures for this work. It may be inferred that at (300^{o}C, 350^{o}C 400^{o}C, the crystalline phase of the catalyst is pure anatase whereas a further increment to 450^{o}C might have resulted into a mixed anatase and rutile TiO_2 NPs phase, which is capable of reducing its photocatalytic capability of degrading methyl red dye.

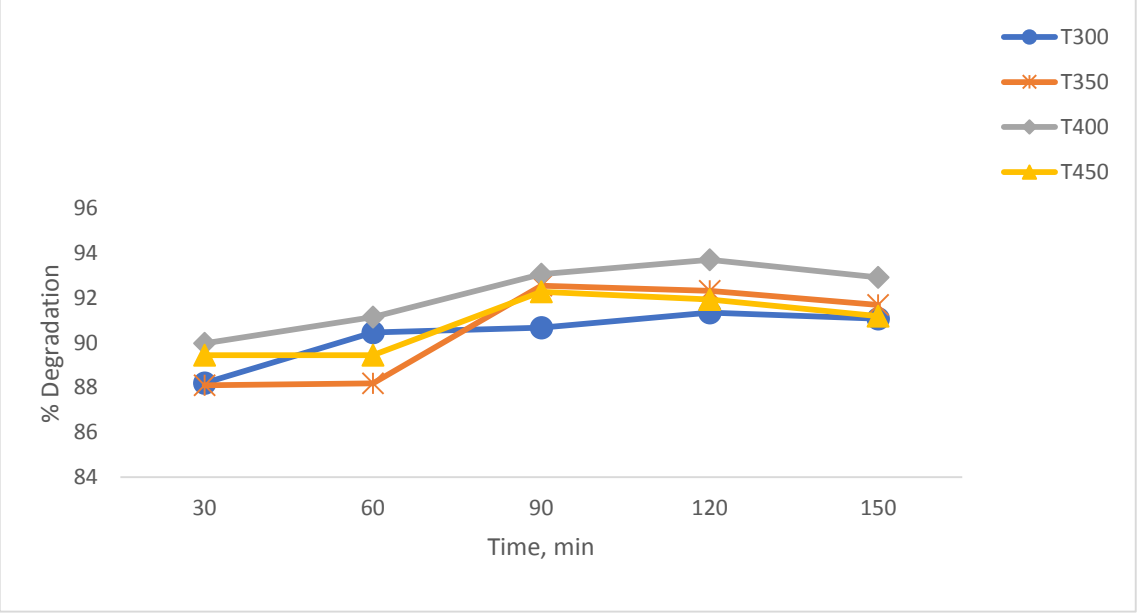

Figure 4.1(a): Effect of calcination temperature on degradation of methyl red dye (Green TiO_2 NPs)

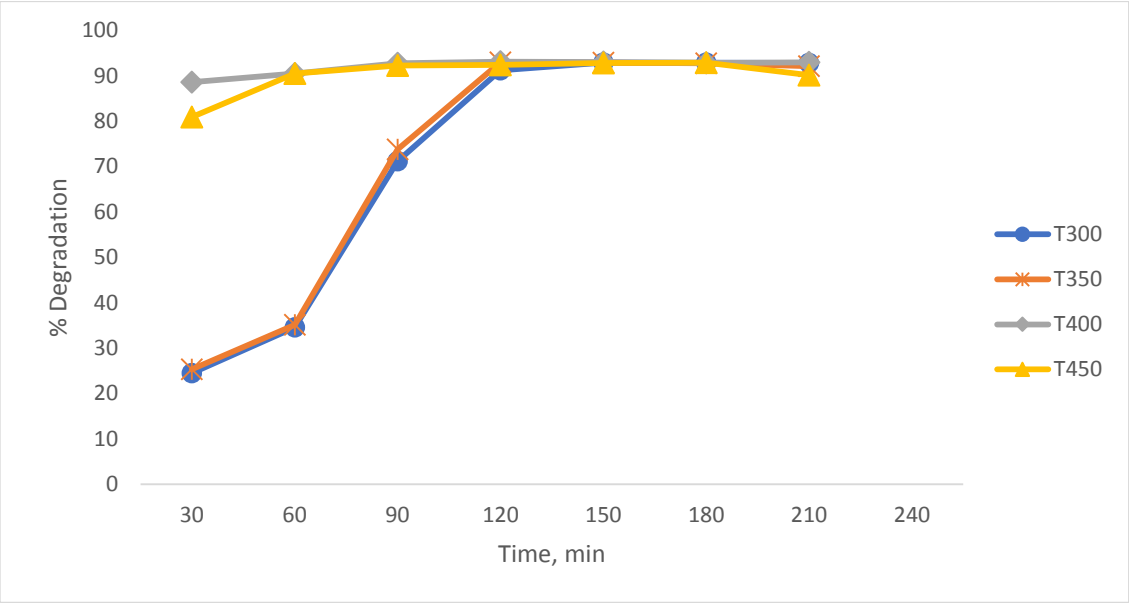

Figure 4.1(b): Effect of calcination temperature on degradation of methyl red dye (Sol-gel TiO_2 NPs)

4.3 Characterization of TiO_2 NPs

It is paramount to study the characteristics of the prepared TiO_2 NPs. Characterization techniques for the particles size and crystallinity, surface area and porosity, morphology, functional groups were considered and reported.

4.3.1 Ultra violet visible spectroscopy (UV-vis Spectroscopy)

The band gap energy (B_g) of TiO_2 NP is a key criterium that determine the effectiveness of the catalyst and its use in photocatalytic experiments. Research shows that the default B_g of TiO_2 is 3 eV for the Rutile phase and 3.2 eV for the anatase phase, which is very efficient for its photocatalytic activeness.

The as synthesized green and Sol-gel TiO_2 NPs were carefully analyzed using a Shimadzu UV-Visible Spectrophotometer (UV-1800 series) in the range 800-200 nm.

The absorbance and wavelength of the semiconductor was utilized to determine its B_g, with the aid of the Tauc plots.

The Tauc energy bang gap plots for the green TiO_2 NPs and the Sol-gel TiO_2 NPs are presented in Figure 4.2(a) and (b) correspondingly. the bang gap energy of the green TiO_2 NPs is seen to be 3.0 eV while that of the sol-gel TiO_2 NPs is 3.1 eV.

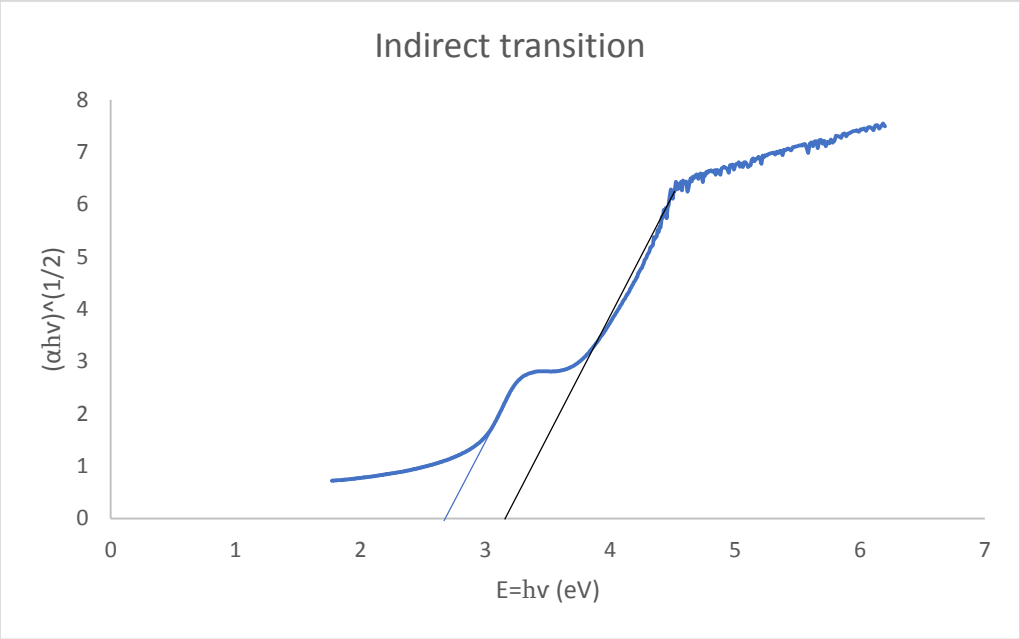

Figure 4.2(a): Tauc energy band gap plot (indirect transition) for green TiO_2 NPs

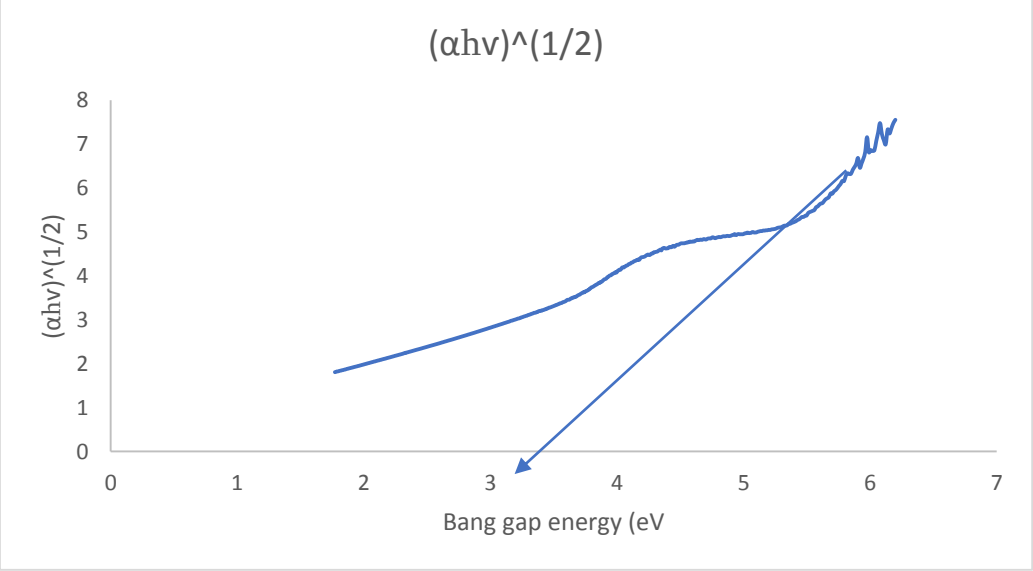

Figure 4.2(b): Tauc Energy band gap plot (indirect transition) for Sol-gel TiO_2 NPs

4.3.2 Fourier transform infrared (FTIR)

FTIR was employed to study the functional group of the synthesized catalysts. The presence of the characteristic peaks in the FTIR spectra of the Sol-gel TiO_2 NPs as shown in Figure 4.3(a) suggests the presence of various functional groups and contaminants on TiO_2 NPs surface. These functional groups might include hydroxyl groups, organic contaminants, carbonyl-containing species, aliphatic compounds, amine groups, silicates, and TiO_2 itself.

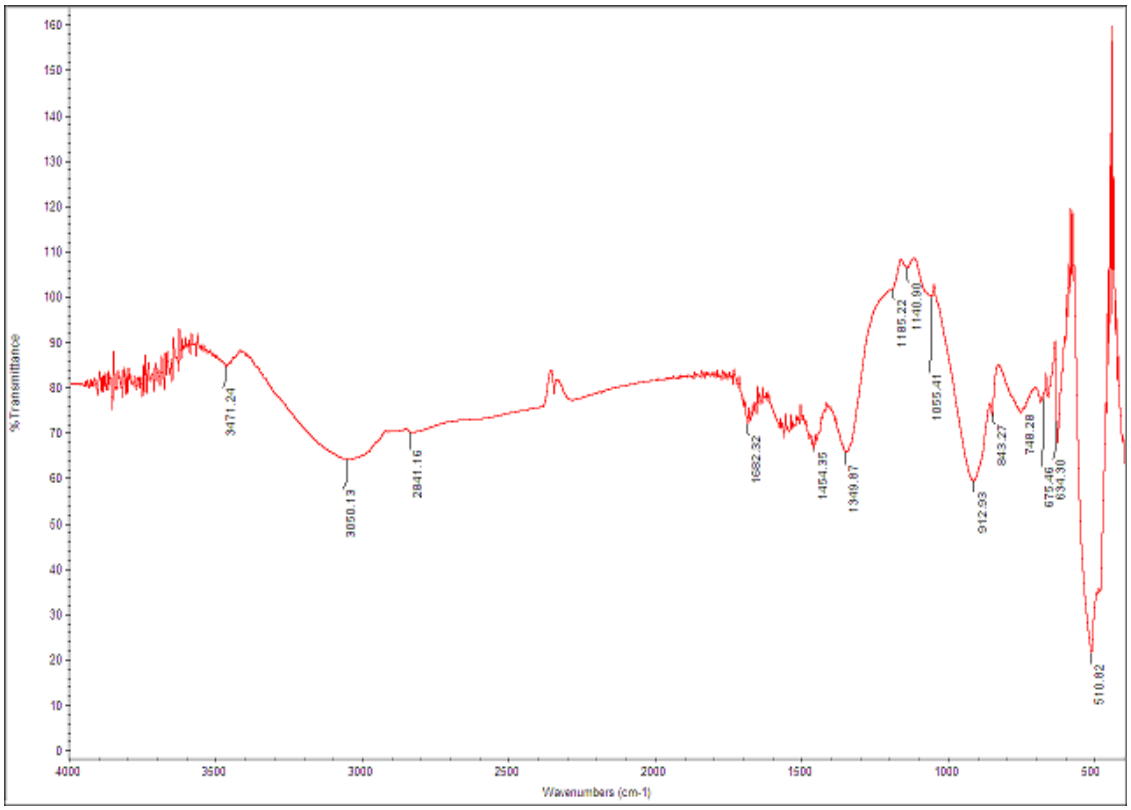

Figure 4.3(a): FTIR spectra of the sol-gel TiO_2 NPs

Several bands were observed at wavelengths 3471.24, 3050.13, 2841.16, 1682.32, 1454.35, 1349.87, 1185.22, 1140.90, 1055.41, 912.93 cm^{-1}.

The wavelength at 3471.24 cm^{-1} is attributed to the stretching vibrations of O-H bond, due to hydroxyl groups (-OH) on surface of the TiO_2 NPs. These hydroxyl groups are

often associated with adsorbed water molecules or residual organic compounds (Subhapriya and Gomathipriya, 2018).

The band at 3050.13 and 2841.16 cm^{-1} respectively may be associated with the stretching vibrations of the C-H bond. This suggests the presence of organic contaminants or carbon-based species attached toTiO_2 NPs.

The band at 1682.32 cm^{-1} is typically accredited to the stretch vibrations of the carbonyl group (C=O). It suggests the presence of carboxylate groups (COO-) or other carbonyl-containing species attached to TiO_2 NPs. The 1454.35 cm^{-1} band corresponds to the bending vibrations of the methyl group (-CH_3) or other aliphatic carbon-hydrogen bonds. It suggests the presence of aliphatic compounds or contaminants.

And the band at 912.93 cm^{-1} corresponds to the stretching vibrations of the Ti-O bond, showed the presence of TiO_2 in the NPs. This result agrees with the report of Subhapriya and Gomathipriya (2018), who juxtaposed that, peaks below 1200 cm^{-1} are as a result of Ti-O-Ti vibrations.

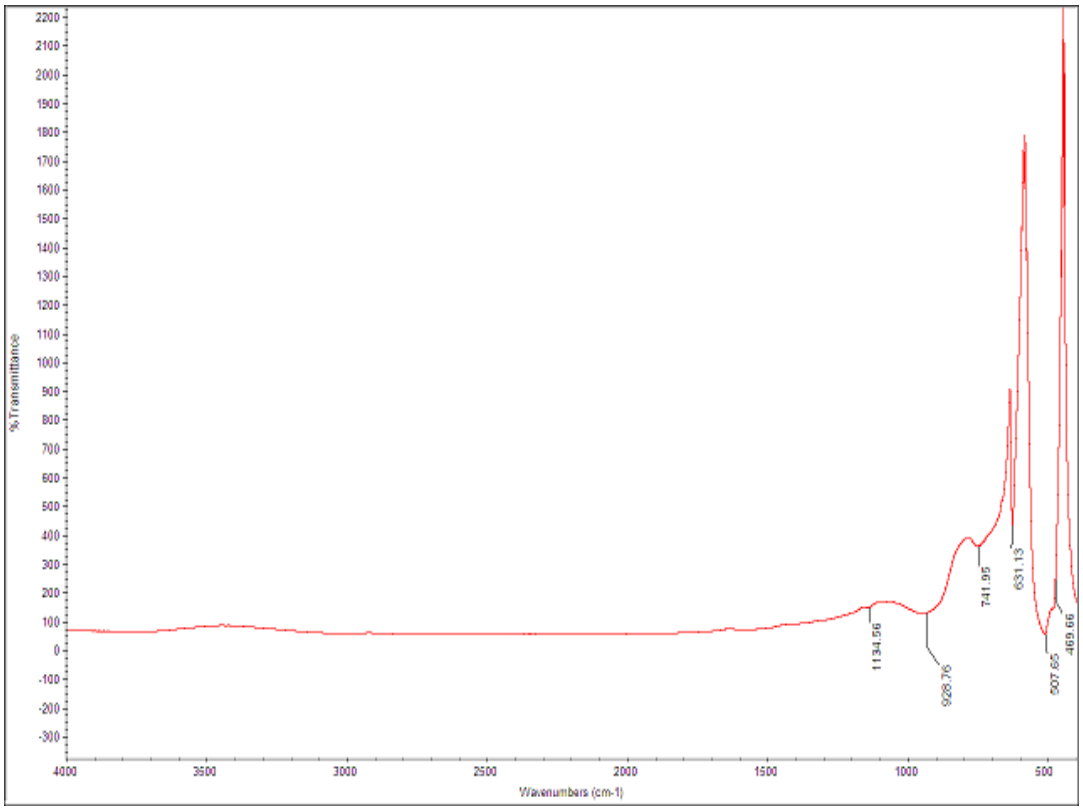

Figure 4.3(b): FTIR spectra of the green (*Delonix regia*) synthesized TiO_2 NPs

Similarly, FTIR spectra of green prepared TiO_2 NPs is as shown in Figure 4.3(b) and the interpretation presented. Infrared bands observed at 1134.56, 928.76, 741.95, 631.13 and 507.65 cm^{-1} respectively.

Peak 1134.56 cm^{-1} suggests occurrence of Ti-O bonds. This peak is characteristic of TiO_2 and indicates the stretching vibration of Ti-O bonds in the NPs. It confirms the formation of TiO_2 nanoparticles in the green synthesis process. The peak at 928.76 cm^{-1} is likely associated with Ti-OH bending vibrations. It indicates the presence of hydroxyl (OH) groups attached to the TiO_2 NPs. These hydroxyl groups might be derived from the phytochemicals present in the *Delonix regia* leaf extracts or possibly from adsorbed water on the nanoparticle surface.

The absorption peak at 741.95 cm^{-1} can be accredited to the vibrations of O-Ti-O bonds. This peak provides further evidence of the presence of TiO_2 NPs, as it corresponds to characteristic vibrations associated with the nanoparticle structure.

The peak at 631.13 cm^{-1} is may be related to the Ti-O-Ti bending vibrations. It indicates the presence of Ti-O-Ti bonds, which are commonly observed in TiO_2 materials. This peak confirms the formation of TiO_2 NPs and suggests a well-defined structure.

And the absorption peak at 507.65 cm^{-1} is typically associated with the stretching vibrations of Ti-O bonds. This peak further confirms the presence of TiO_2 NPs and suggests the crystalline nature of the material. Abisharani *et al.,* (2019) reported that the peaks below 700 cm^{-1} are largely controlled by the presence of leaf extract.

4.3.3 X-ray diffraction (XRD) analysis

The average particle size, crystallinity and crystallite size of the catalysts was investigated from XRD pattern on Figure 4.4. the XRD pattern of the synthesized green TiO_2 NPs revealed peaks at 2Theta (2θ) values of 27.534^0, 36.08^0, and 54.29^0 respectively. The XRD spectra shows that the TiO_2 NPs are crystalline in nature of rutile planes 110, 101, and 211 of TiO_2 respectively.

The observed patterns at stated 2θ values corresponded with the rutile TiO_2 and the results agreed with the Joint Committee on Powder Diff raction Standards (JCPDS) No. 04-007-4874.

Green TiO_2 NPs average crystallite size was estimated from equation 4.1to be 22.61 nm. This is similar to 25 nm average crystallite size of *Trigonella foenum-graecum* extract synthesized TiO_2 NPs reported by Subhapriya and Gomathipriya (2018).

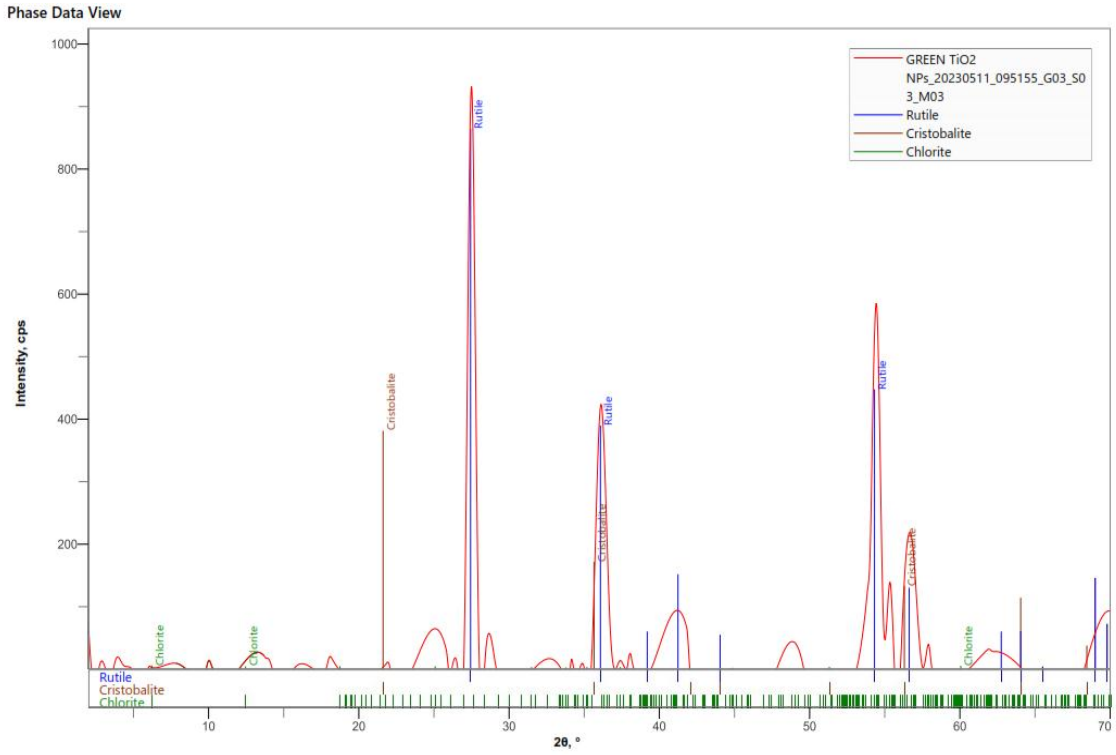

Figure 4.4: XRD pattern of green (*Delonix regia*) synthesized TiO_2 NPs

4.3.4 Scanning electron microscopy/Energy dispersion X-ray (SEM/EDX) analysis

The surface structure and morphology of the both synthesized TiO_2 NPs was studied using SEM and EDX was used to confirm the percentages of the various elemental components of the NPs.

Figure 4.5(a) shows the SEM micrograph of the green synthesized TiO_2 NPs. The particles are agglomerated and porous in nature. The morphology can be seen to be irregular whereas some particles are spherical 5 μm average particle diameter. This result corroborates the work of Velayutham *et al.*, 2011.

The EDX of the green TiO_2 NPs as shown in Figure 4.5(a) indicates the presence of 0.8265 wt.% of Titanium (Ti), 0.1535 wt.% of Oxygen (O_2) and some 0.02 wt.% Carbon (C) impurity which may be attributed to the phytochemical content of the

Delonix regia leaf extract. This infers that the catalyst is highly composed of TiO_2 NPs.

Figure 4.5(b) shows the SEM/EDX of the sol-gel synthesized TiO_2 NPs. The SEM micrograph displays a large porous and well agglomerated TiO_2 aggregate particles of spherical shapes of 10 μm average particle diameter.

The EDX shows the presence of 0.7975 wt.% Titanium and 0.2025 wt.% Oxygen with 1.2 and 0.1 Kev energy levels respectively.

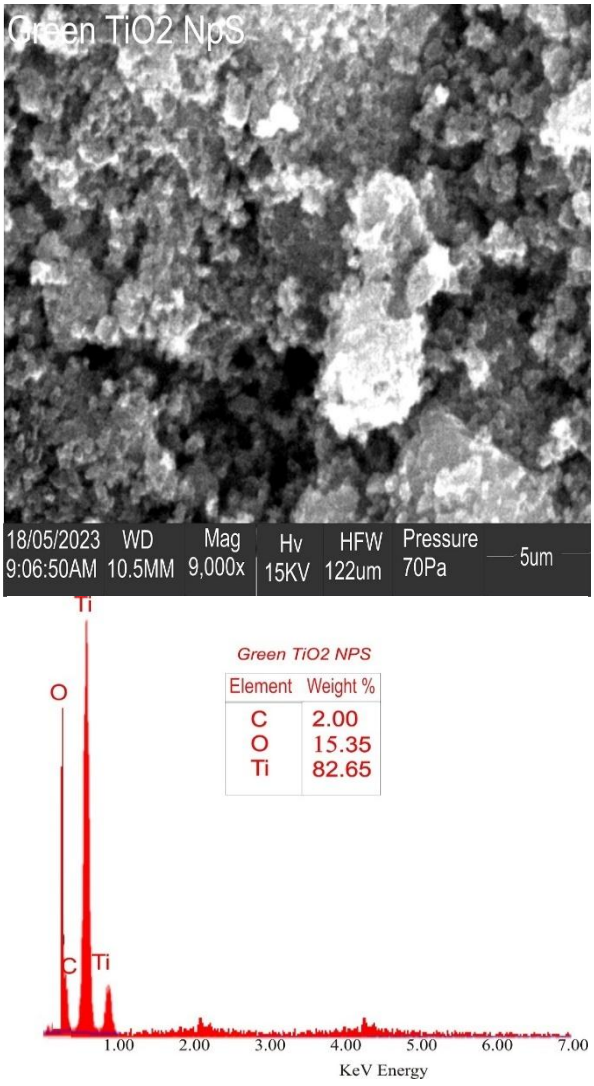

Figure 4.5(a): SEM/EDX micrograph of the green synthesized (*Delonix regia*) TiO_2 NPs

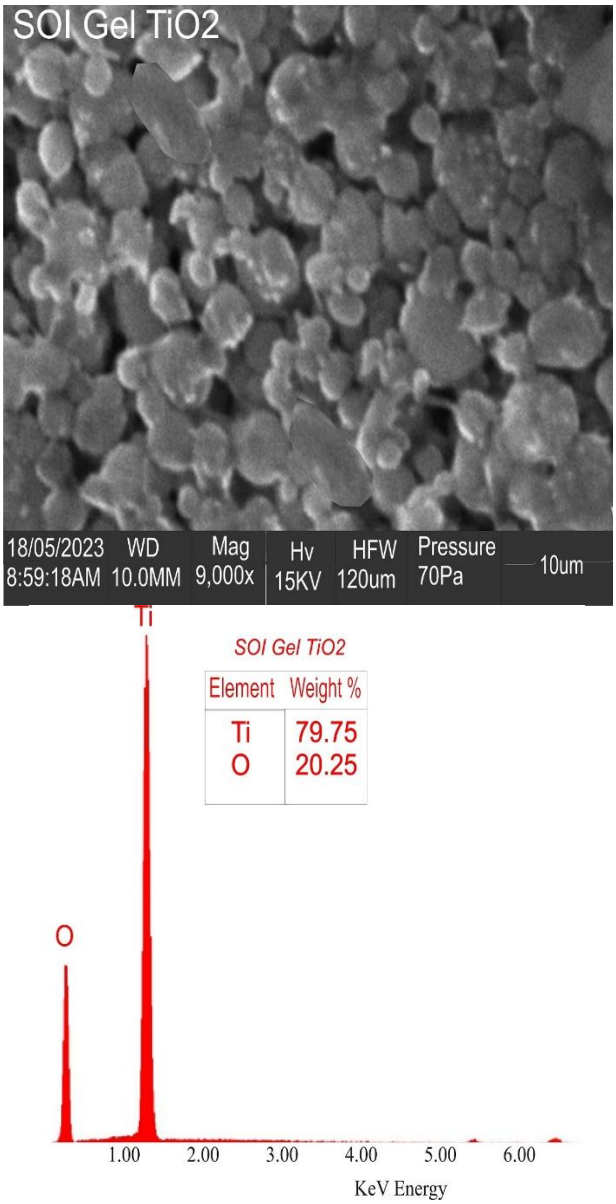

Figure 4.5(b): SEM/EDX micrograph of the Sol-gel synthesized TiO_2 NPs

4.3.5 Brunauer Emmet Teller (BET) surface area

The synthesized photocatalyst were characterized to determine the developed surface area via Brunauer-Emmet-Teller (BET) and pores sizes from the Barrett-Joyner-Hallenda (BJH). The investigations were performed using N_2 adsorption/desorption measurements at 273K and the adsorption isotherm is shown in Figure 5.6. P/P_o is the relative partial pressure.

The N_2 adsorption/desorption isotherm of TiO_2 NPs is classified as Type-I isotherm and its characteristic of porous solids.

Both figures depict a Type-I monolayer adsorption isotherm which is a typical characteristic of a microporous material with diameter less than 2 nm. The BET surface area was calculated to be 371.390 m^2/g with correlation coefficient, R^2, of 0.993002. the BJH pore diameter of the catalyst is 2.137 nm for the green TiO_2 NPs while the BET surface area of the Sol-gel TiO_2 NPs is 336.463 m^2/g with R^2 value of 0.996314 and the BJH pore diameter is 2.128 nm.

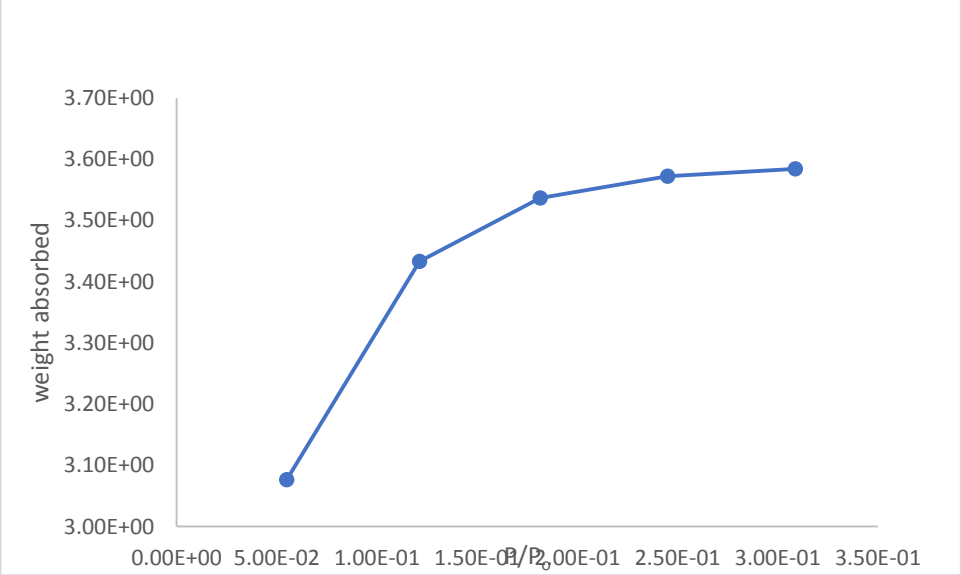

Figure 4.6: Type-I adsorption isotherm of TiO_2 NPs

4.4 Preliminary Studies on the TiO_2 NPs Degradation of Methyl Red Dye Solution

Initial investigations were carried out using the freshly synthesized photocatalysts to assess their efficacy in degrading methyl red dye solution. Two types of experiments, namely photolysis (where the reaction occurred under solar irradiation without the presence of catalysts) and adsorption (where the reaction took place with the TiO_2 NPs catalyst in a dark environment), were conducted. The findings are presented in Table

4.3. A consistent catalyst dosage of 0.1 g and a reaction duration of 3 hours were maintained throughout all the experiments.

The results indicate that in the case of photolysis, methyl red degradation under solar irradiation is feasible, albeit at a relatively slow pace. Photolysis is actually able to generate hydroxyl (OH*) radicals which are instrumental in the degradation of organic pollutants. Hence, this indicates that in the absence of a photocatalyst, methyl red dye may remain in solution undegradable for a lengthy period of time.

In the adsorption study in a dark medium, there appears to be zero colour removal of the methyl red dye. It may be inferred that adsorption and desorption of the dye molecules with TiO_2 NPs may be occurring at equilibrium.

However, with the synthesized TiO_2 NPs and in the presence of solar irradiation, a significant reduction in colour was observed, from 45 mg/L to 3.38 mg/L (Sol-gel catalyst) and 3.21 mg/L (green catalyst). This equates to a degradation rate of 92.50% for the Sol-gel TiO_2 NPs and 93.02% for the green TiO_2 NPs.

Therefore, the photocatalytic degradation of methyl red dye was made possible by the photon energy from solar irradiation and the TiO_2 NPs catalyst.

Table 4.3: Preliminary experimental studies with TiO_2 NPs

Activity	Catalyst	% Degradation
Photolysis	Nil	2.86
Adsorption	Sol-gel	Nil
	Green catalyst	Nil
Photocatalysis	Sol-gel	92.50
	Green catalyst	93.02

Note; Initial Concentration of Simulated Dye Solution: 45 mg/L

4.5 Photocatalytic Experiments

The following parameters related to photocatalytic degradation were investigated: catalyst dosage, pH of the dye solution, concentration of the dye solution, and reaction time. The results obtained for each parameter are presented below:

4.5.1 Effect of catalyst dosage on photocatalytic degradation of methyl red dye solution

Photocatalyst dosage used in the degradation reaction plays a crucial part in determining the optimal amount required for complete reaction, specifically in the case of photocatalysis with TiO_2 NPs. As depicted in Figure 4.2(a) and (b), the degradation colour removal effectiveness of both the Sol-gel and green catalysts exhibited a proportional increase with the incremental dosage of catalysts ranging from 0.1 g to 0.3 g. This observation suggests that a sufficient amount of catalyst is needed generate sufficient hydroxyl radicals (*OH), which play a great part in the oxidation-reduction process responsible for the degradation of organic pollutant molecules. This indicates a

proportional increment in the degradation rate and is described as the heterogeneous regime (Reza *et al.*, 2017).

Furthermore, when the catalyst dosage was increased up to 0.4 g, the photocatalytic efficiency of both catalysts declined. The finding supports report in previous work reported by Suresh *et al*., 2018, which state that exceeding the optimal photocatalyst dose leads to a saturation point where the absorptive sites become inaccessible to photon energy. As a result, the solution becomes turbid and over-saturated with the catalyst, hindering light penetration and impeding the progression of the photocatalytic reaction. Consequently, this decreases in light availability result in a reduction in the degradation rate.

Therefore, for the green catalyst, the optimum dosage was 0.2 g while for the Sol-gel prepared catalyst it was 0.3 g.

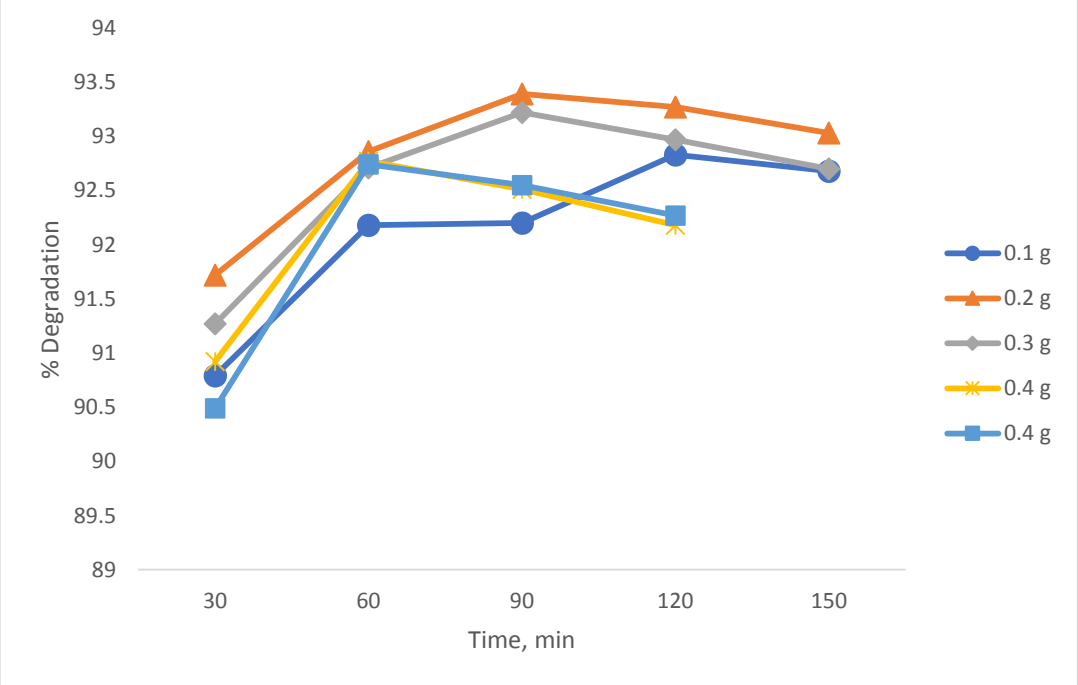

Figure 4.7(a): Effect of dosage on degradation of methyl red dye (green TiO_2 NPs)

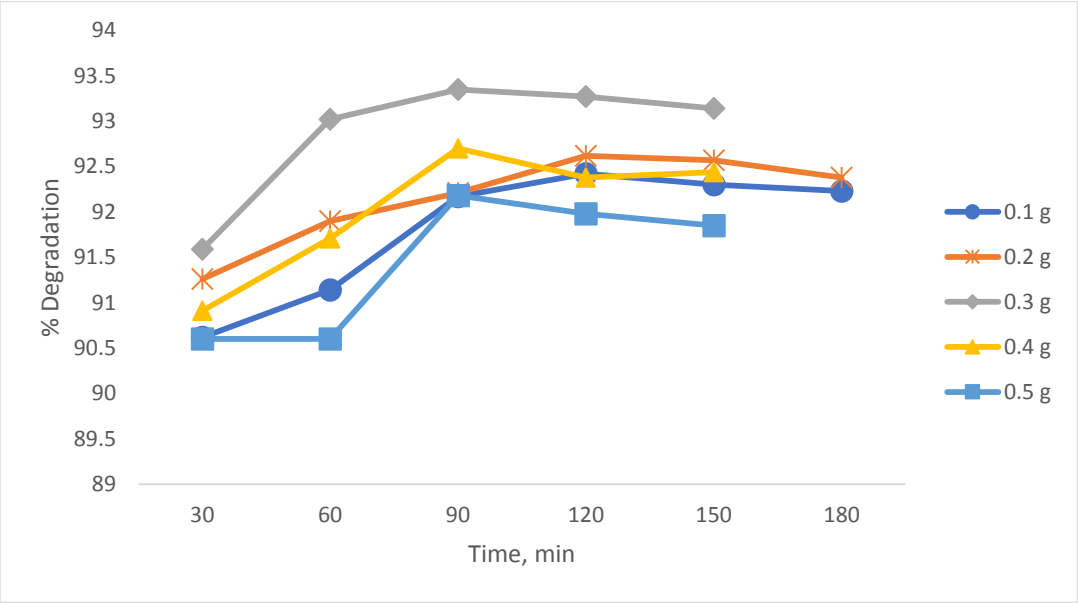

Figure 4.7(b): Effect of dosage on degradation of methyl red dye (Sol-gel TiO_2 NPs)

4.5.2 Effect of initial concentration of methyl red dye

The influence of dye concentrations, ranging from 10 to 50 mg/L, was examined while keeping the catalyst dosage and reaction time constant. The results, presented in Figures 4.3(a) and (b) for the green and Sol-gel TiO_2 catalysts respectively, demonstrate that an increment in dye concentration results in a decrease in degradation efficiency for both types of catalysts. It is evident that the percentage degradation decreased as the concentration rises, despite maintaining a consistent catalyst dosage. This deduction suggests that the active sites of a catalyst become less available as concentration of dye pollutant increased, and the degradation ability of the photocatalyst diminished.

As seen in figures 4.3 (a) and (b), there was a proportional increase in the percentage degradation as reaction time increased. At lower concentrations of 10 mg/L and 20 mg/L, it took 60 min and 99% of the dye was removed from solution. However, at a higher dye concentration of 40 mg/L and 50 mg/L, there was a decline in the percentage

degradation. This means the catalyst active sites were limited relative to the available catalyst dose. Nonetheless, it is possible that more dye molecules were degraded at higher concentrations of 40 mg/L to 50 mg/L, as observed in the photocatalytic degradation of 2,4-dichlorophenoxyacetic acid by Akpan and Hameed (2011).

The decrease in methyl red degradation as its concentration increases may be attributed to adsorption of dye molecules on the TiO_2 NPs surface and more significant amount of light irradiation is absorbed by the methyl red dye molecules instead of the photocatalyst, hence reducing the diffusion capacity of the photons to activate the generation hydroxyl radicals (Reza *et al.*, 2017).

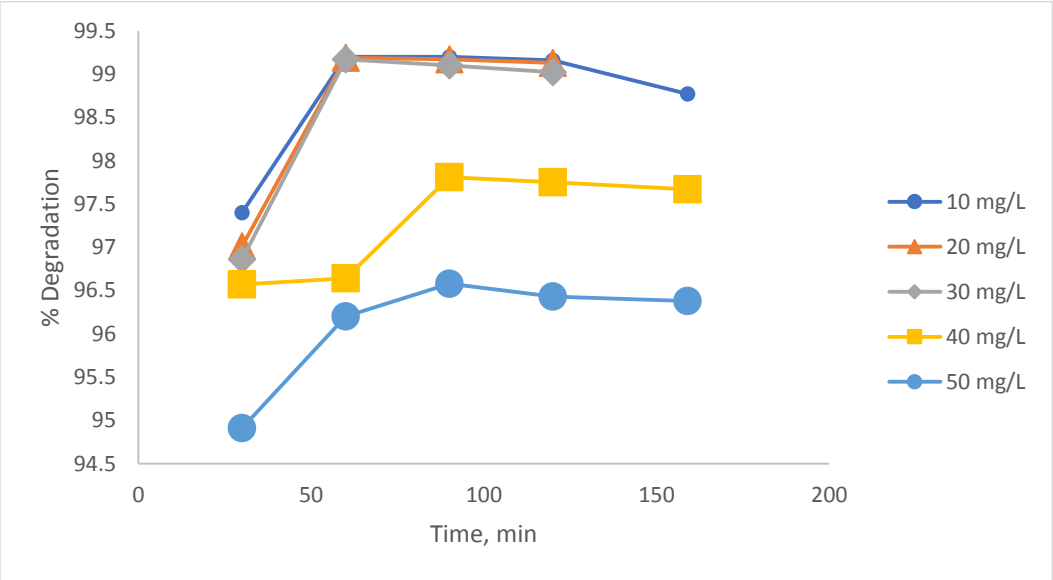

Figure 4.8(a): Effect of initial concentration on degradation of methyl red dye (green TiO_2 NPs)

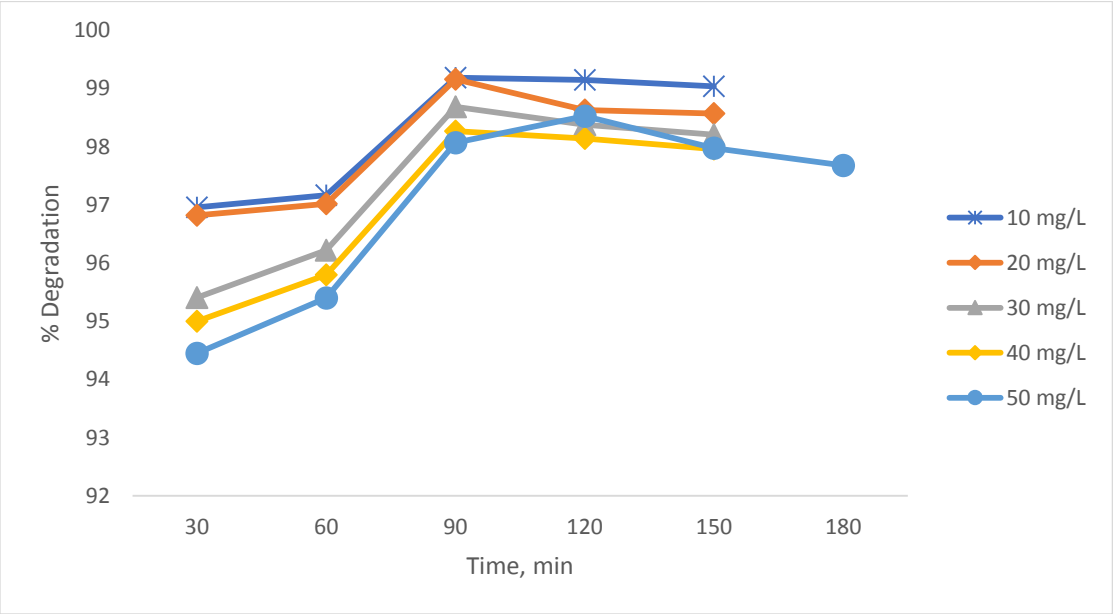

Figure 4.8(b): Effect of initial concentration on the degradation of methyl red dye (Sol-gel TiO_2 NPs)

4.5.3 Effect of pH on degradation of methyl red dye solution

The influence of pH on the photocatalytic colour removal of methyl red dye in solution was investigated across the pH range of 2 to 10. The results, illustrated in Figures 4.4(a) and (b) for the green and Sol-gel TiO_2 NPs catalysts respectively, indicate that an acidic pH promotes better dye degradation compared to an alkaline pH.

In the acidic range, the Sol-gel and green catalyst surfaces acquire a positive charge. This results in a higher production of hydroxyl radicals (OH*) with improved oxidative capability, hence improves the photocatalytic effectiveness (Yasmina *et al.*, 2014). Conversely, in the alkaline range, the photocatalyst active sites become negatively excited, which subsequently reduces the rate at which the dye molecules degrade (Suresh *et al.*, 2018)

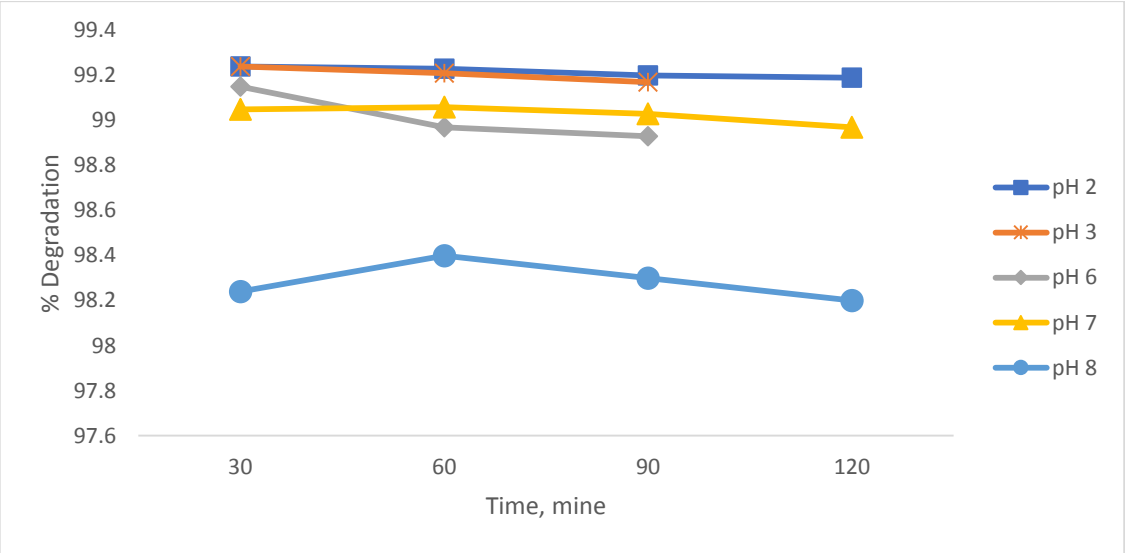

Figure 4.9(a): Effect of pH on the degradation of methyl red dye solution (Green TiO_2 NPs)

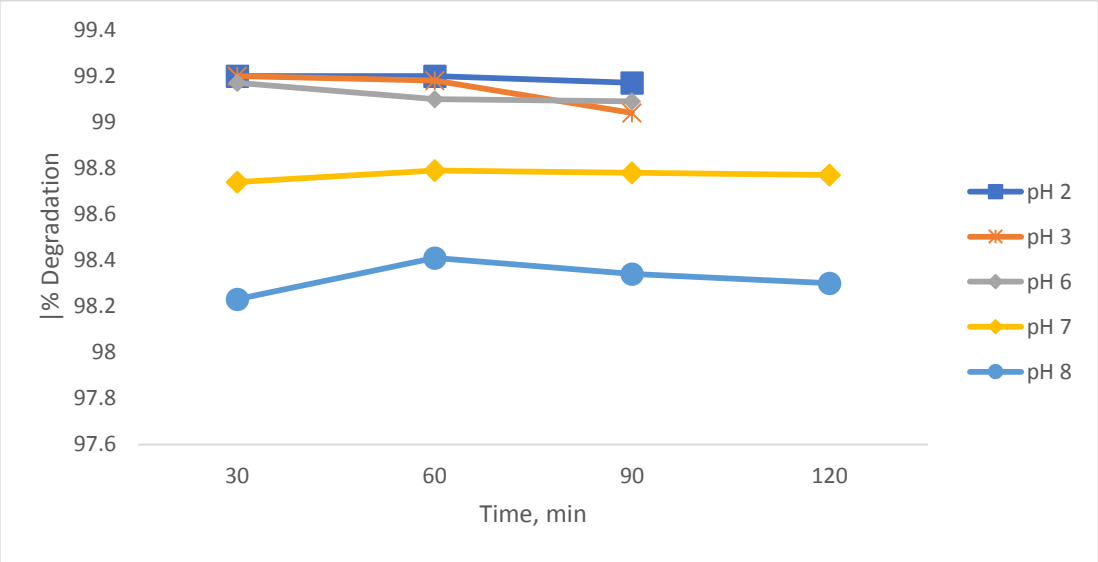

Figure 4.9(b): Effect of pH on the degradation of methyl red dye solution (Sol-gel TiO_2 NPs)

4.6 Reaction Kinetics

The reaction kinetics of both green and Sol-gel prepared TiO_2 NPs was studied to ascertain the quantitative degradation of the dye at the various concentration range from 10 mg/L to 50 mg/L in solution respectively. This was evaluated over 150 min period,

0.1 g catalyst dosage and pH 3. The experimental data fitted by pseudo-first-order kinetics was plotted and the results are presented on Table 4.4.

For the green TiO_2 NPs photocatalytic degradation of methyl red dye, the correlation coefficient is the range 0.6436-0.8353 whereas that of the Sol-gel is in the range 0.8303-0.9527 for all concentrations considered in the study and it indicates a satisfactory fitting for both data as shown in the plot $ln\frac{C_o}{C_t}$ versus Time (T) for the green and sol-gel TiO_2 NPs degradation of methyl red dye (Figures 4.10 (a) and (b)).

It can be seen that with the increment of dye concentration, the degradation rate constant reduces as well. This indicates a transition from a kinetic control regime at lower dye concentration to a mass transfer limitation at higher dye concentrations. Also, there is an increase in the number of intermediate products, hydroxyl radicals generated then became limiting reactants, hence reducing the degradation rate.

Table 4.4: Kinetics parameters for the photocatalytic degradation of methyl red dye

Initial concentration(mg/L)	Rate equation	Constant (K)	Correlation coefficient (R^2)	Catalyst type
10	y = 0.3952x + 3.4754	0.3952	0.6436	green
20	y = 0.2797x + 3.6572	0.2797	0.7617	green
30	y = 0.4075x + 3.3798	0.4075	0.7095	green
40	y = 0.13x + 3.2378	0.13	0.8353	green
50	y = 0.0856x + 2.9982	0.0856	0.7198	green
10	y = 0.3852x + 3.1018	0.3852	0.8303	Sol-gel
20	y = 0.3385x + 3.0398	0.3385	0.9013	Sol-gel
30	y = 0.3357x + 2.7603	0.3357	0.9184	Sol-gel
40	y = 0.2943x + 2.7367	0.2943	0.8712	Sol-gel
50	y = 0.352x + 2.5247	0.352	0.9527	Sol-gel

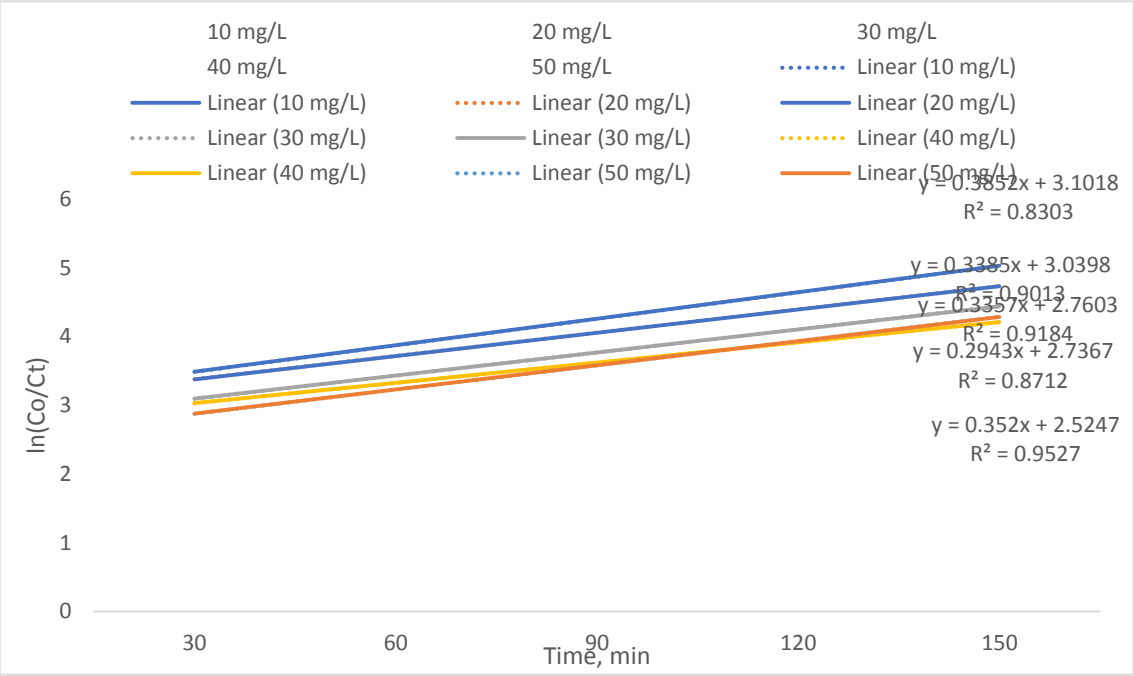

Figure 4.10(a): First order plot for the photocatalytic degradation of methyl red dye

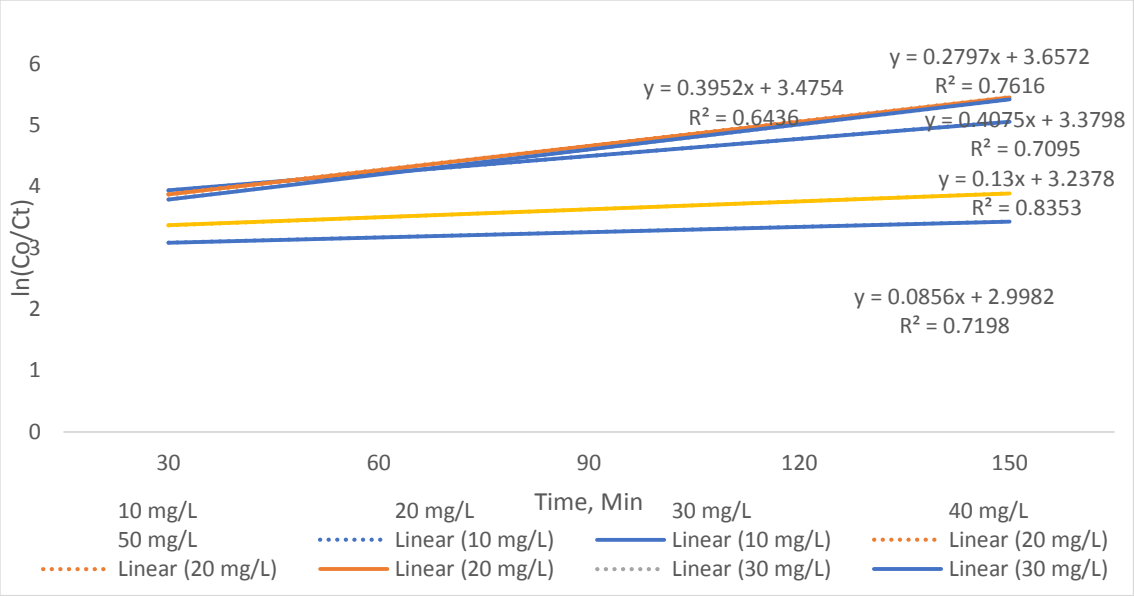

(green TiO_2 NPs)

Figure 4.10(b): First order plot for the photocatalytic degradation of methyl red dye (Sol-gel TiO_2 NPs)

CHAPTER FIVE

5.0 CONCLUSION AND RECOMMENDATIONS

5.1 Conclusion

In this research, TiO_2 nanoparticles (NPs) were successfully synthesized using two methods: the green method and the Sol-gel method. The green method involved the utilization of *Delonix regia* plant extract, which contains valuable phytochemicals and metabolites essential for the reduction and capping of the nanoparticles. These plant-derived components played a critical function in the formation and stabilization of the TiO_2 NPs during the synthesis process.

The synthesized TiO_2 NPs are highly porous and of spherical shapes. Both synthesized photocatalysts demonstrated excellent photocatalytic capability in methyl red dye degradation. There was a significant colour removal of 92% and 93% for the Sol-gel TiO_2 NPs and green TiO_2 NPs respectively.

It is important to study the photocatalytic degradation factors like catalyst dosage, initial dye concentration, pH and calcination temperature. In this study, the synthesized TiO_2 NPs performed better in a lower pH medium (acidic), the optimum dosage was determined to be between 0.2 g and 0.3 g.

5.2 Recommendations

For a higher degradation efficiency of photocatalysts, its therefore recommended that;

i. Use UV lamps to conduct the photocatalytic experiments for optimum catalyst performance.
ii. The green synthesized catalysts should be doped with metals to further reduce band gap and improve their efficiency in photocatalytic applications

iii. Design a continuous process photocatalytic reactor which can be applicable for industries handle real life situations.

5.3 Contributions to Knowledge

At the successful completion of this research, the following are the knowledge contributions achieved;

i. *Delonix. regia* leaf extract can be employed a reduction and stabilizing agent to reduce Titanium Butoxide into 22.6 nm Titanium dioxide Nanoparticles which are useful in the degradation of methyl red dye solution.

ii. The study compared a chemical and green methods of synthesizing Titanium dioxide nanoparticles and was able to demonstrate that the green method is cheaper and more effective in the degradation of methyl red dye to 93.02 % as against the 92.50 % of the chemical method. This method is less toxic as the nanoparticle reducing and stabilizing agents were obtained from the plant extract.

iii. Solar irradiation is a capable, viable and economical replacement for Ultraviolet light in providing enough photon energy for photocatalysis. It promoted the degradation of methyl red dye up to 92.50 % and 93.02 % for the sol-gel and green TiO_2 nanoparticles respectively.

iv. Solar irradiation is capable and viable replacement for Ultraviolet light in providing enough photon energy for photocatalysis.

v. The study also has contributed to the knowledge base of green synthesis technology, nanotechnology, photocatalysis and wastewater treatment.

REFERENCES

Abbasi, I. (2021). Titanium Dioxide Nanoparticles: Industrial Applications and Developments. *AzoNano*, 1-8.

Abdellah,M. H., Nosier,S. A., EL Shazly, A. H., & Mubarak,A.A.(2018).Photocatalytic decolorization of methylene blue using TiO_2/UV system enhanced by air sparging. *Alexandria Engineering Journal*. doi:doi.org/10.1016/j.aej.2018.07.018

Abhang, R. M., Kumar, D., & Taralkar, S. V. (2011). Design of Photocatalytic Reactor for Degradation of Phenol in Wastewater. *International Journal of Chemical Engineering and Apllications, 2*(5), 337-341.

Abisharani, J. M., Devikala, S., Dinesh Kumar, R., Arthanareeswari, M., & Kamaraj, P. (2019). Green synthesis of TiO_2 Nanoparticles using Cucurbita pepo seeds extract. *Materials Today: Proceedings, 14*, 302-307.

Akpan, U. G., & Hameed, B. H. (2009). Parameters affecting the photocatalytic degradation of dyes using TiO_2-based photocatalysts: A review. *Journal of Hazardous Materials, 170*, 520–529.

Akpan, U. G. (2011). *Synthesis, Characterization and Activity of Titanium Dioxide Based (Ca, Ce, W)-TiO_2 Photocatalysts for Degradation of Dye and Pesticide.* Universiti Sains Malaysia.

Amanulla, A. M., & Sundaram, R. (2019). Green synthesis of TiO_2 nanoparticles using orange peel extract for antibacterial, cytotoxicity and humidity sensor applications. *Materials Today; Proceedings, 8*, 323-331.

Ameta, R., Benjamin, S., Ameta, A., & Ameta, S. C. (2013). Photocatalytic Degradation of Organic Pollutants: A Review. *Materials Science Forum, 734*, 247-272. doi:10.4028/www.scientific.net/MSF.734.247

Amini, M., & Ashrafi, M. (2016). Photocatalytic degradation of some organic dyes under solar light irradiation using TiO_2 and ZnO nanoparticles. *Nano Chemical Resources,* 1(1), 79-86.

Aravind, M., Amalanathan, M., & Sony M. M. (2021). Synthesis of TiO_2 nanoparticles by chemical and green synthesis methods and their multifaceted properties. *SN Applied Sciences, 3*(409). doi:10.1007/s42452-021-04281-5

Ashraf, M. W. (2021). Removal of methylene blue dye from wastewater by using supported liquid memebrane technology. *Polish Journal of Chemical Technology,* 1*8*(2), 1-5.

Balkus, K. J. (2013). Metal Oxide Nanotube, Nanorod, and Quantum Dot Photocatalysis. In K. J. Balkus, *Catalysis by Nanoparticles.* Texas, 213-244.

Bento, R. T., & Pillis, M. F. (2018). Titanium Dioxide Films for Photocatalytic Degradation of Methyl Orange Dye. *Material for a Sustainable Environment,* 211-225.

Chauhan, R. P., Gupta, C., & Prakash, D. (2012). Methodological advancements in green nanotechnology and their applications in biological synthesis of herbal nanoparticles. *International Journal of Bioassays*, 1(7), 6-10.

Chequer, F. M., de Oliveira, G. A., Ferraz, E. R., Cardoso, J. C., Zanoni, M. V., & de Oliveira, D. P. (2013). Textile dyes; Dyeing process and Environmental impact. *Eco-Friendly Textile Dyeing and Finishing*, 151-176.

Colmenares, J. C., & Luque, R. (2014). Heterogeneous photocatalytic nanomaterials; Prospects and challenges in selective transformations of biomass derived compounds. *Royal society of chemistry, 43*, 765-778.

de Lasa, H., Serrano, B., & Salaices, M. (2005). *Photocalytic Reaction Engineering.* New York: Springer. doi:10.1007/978-0-387-27591-8

Dobruka, R. (2017). Synthesis of Titanium Dioxide Nanoparticles Using Echinacea purpurea Synthesis of Titanium Dioxide Nanoparticles Using Echinacea purpurea. *Iranian Journal of Pharmaceutical Research, 16*(2), 756-762.

Ghime, D., & GHosh, P. (2020). Advanced Oxidation Processes; A powerful treatment option for the removal of reclacitrant organic compounds. *Advanced Oxidation processes- Applications, Trends, and Prospects*, 1-12.

Goutam, S. P., Saxena, G., Singh, V., Yadav, A. K., Bharagava, R. N., & Thapa, K. P. (2017). Green synthesis of TiO_2 nanoparticles using leaf extracts of Jatropha curcas L. for photocatalytic degradation of tannery wastewater. *Chemical Engineering Journal*, 1-42. doi:doi.org/10.1016/j.cej.2017.12.029

Innalegwu, D. A., Uyi, E. J., Emmanuel, M. B., & Ufedo, E. Q. (2017). Quantitative Phytochemical and Antibacterial Efficacy of Fractions of Terminalia microptera Leaf. *American Journal of Pharmacy and Pharmacology*, *5*(4), 35-40.

Irshad, M. A., Nawaz, R., Rehman, M. Z., Imran, M., Ahmad, M. J., Ahmad, S., Ali, S. (2020). Synthesis and characterization of Titanium dioxide nanoparticlse by chemical and green methods and their antifugal activity against wheat rust. *Chemosphere*, 1-20.

Irshrad, M. A., Nawaz, R., Rheman, M. Z., Andrees, M., Rizwan, M., Ali, S., Saleem, S. (2021). Synthesis, characterization and advanced sustainable applications of titanium dioxide nanoparticles: A review. *Ecotoxicology and Environmental Safety, 212*, 111978. doi:10.1016/j.ecoenv.2021.111978

Kashale, A. A., & Ghule, A. V. (2016). Biomediated green synthesis of TiO2 nanoparticles for lithium ion battery application. *Composites Part B: Engineering*, 297-304.

Kim, M. G., Kang, J. M., Lee, J. E., Kim, K. S., Kim, K. H., Cho, M., & Lee, S. G. (2021). Effects of Calcination Temperature on the Phase Compostion, Photocatlytic Degradation and Virucidal Activities of TiO_2 Nanopoarticles. *ACS Omega, 6*(16), 10668-10678.

Kumar, P. S., Francis, A. P., & Devasena, T. (2014). Biosynthesized and chemically synthesized Titania Nanoparticles: Comparative Analysis of Antibacterial activity. *Journal of Envrionmental Nanotechnology.*, *3*(3),73-81. doi:10.13074/jent.2014.09.143098

Lellis, B., Fávaro-Polonio, C. Z., Pamphile, J. A., & Polonio, J. C. (2019). Effects of textile dyes on health and the environment and bioremediation potential of living organisms. *Biotechnology Research and Innovation*, 1-16.

Macwan, D. P., Dave, P. N., & Chaturvedi, S. (2011). A review on nano-TiO2 sol-gel type syntheses and its applications. *Journal of Matter Science, 46*, 3669-3686.

Makula, P., Pacia, M., & Macyk, W. (2018). How to correctly Determine the BAnd Gap Energy of Modified Semiconductor Photocatalysts Bases on UV-Vis Spectra. *Journal of Physical Chemistry Leterst, 9*(23), 6814-6817.

Moma, J., & Baloyi, J. (2018). Modified Titanium Dioxide for Photocatalytic Applications. In IntechOpen, *Photocatalysts - Applications and Attributes* (pp. 37-56). IntechOpen. doi:http://dx.doi.org/10.5772/intechopen.79374

Marimuthu, S., Rahuman, A. A., Jayaseelan, C., Kirthi, A. V., Santhoshkumar, T., Velayutham, K., M., I. (2013). Acaricidal activity of synthesized titanium dioxide nanoparticles using Calotropis gigantea against Rhipicephalus microplus and Haemaphysalis bispinosa. *Asian Pacific Journal of Tropical Medicine, 6*(9), 682-688.

Mishra, N. S., Reddy, R., A., K., Rani, A., Mukherjee, P., Nawaz, A., & Pinchiah, S. (2017). A Review on Advanced Oxidation Processes for Effective Water Treatment. *Current World Environment, 12*(3), 470-490.

Mohamad, N. A., Arham, N. A., Jai, J., & Hadi, A. (2014). Plant Extract as Reducing Agent in Synthesis of Metallic Nanoparticles: A review. *Advanced Materials Research, 832*, 350-355.

Mondal, S., Roy, N., Laskar, R. A., I. Sk, I., Basu, S., Mandal, D., & A., B. (2011). Biogenic synthesis of Ag, Au and bimetallic Au/Ag alloy nanoparticles using aqueous extract of mahogany leaves. *Colloids and Surfaces. B*, 497-504.

Muthukumar, S., Kalyanasundharam, S., Santhanalakshmi, .., & Jacquline Rosy, P. (2017). Biosynthesis, Characterization of Tio2 Nanoparticles by Using Solanum Xanthocarpum Berry Extract and Their Biomedical and Photocatalytic Activity. *International Journal for Research in Applied Science & Engineering Technology (IJRASET), 5*(12), 738-746.

Nadeem, M., Tungmunnithum, D., Hano, C., Abassi, B. H., Hasmi, S. S., Ahmad, W., & Zahir, A. (2018). The current trends in the green syntheses of titanium oxide nanoparticles and their applications. *Green Chemistry Letters and Reviews, 11*(4), 492-502. doi:10.1080/17518253.2018.1538430

Nyamukamba, P., Okoh, O., Mungondori, H., Taziwa, R., & Zinya, S. (2018). Synthetic Methods for Titanium Dioxide Nanoparticles: A Review. *Material for a Sustainable Environment*, 151 -175. doi:http//dx.doi.org/10.5772/intechopen.75425

Olukani, O., Awotula, A., Osuntoki, A., & Govindwar, S. (2019). Influence of redox mediators and media on methyl red decolorization and its biodegradation by providencia rettgeri. *Applied Sciences, 1*(697), 697.

Philippopoulos, C. J., & Nikolaki, M. D. (2010). Photocatalytic processes on the oxidation of organic compounds in water. *New trends in Technology*, 89-108.

Rafiq, A., Ikram, M., Ali, S., Niaz, F., Khan, M., Khan, Q., & Maqboool, M. (2021). Photocatalytic degradation of dyes using semiconductor photocatalysts to clean industrial water pollution. *Journal of Industrial and Engineering Chemistry*, *97*, 111–128. doi:10.1016/j.jiec.2021.02.017

Rajakumar, G., Rahuman, A. A., Priyamvada, B., Khanna, V. G., Kumar, D. K., & Sujin, P. J. (2012). Eclipta Prostrata leaf aqueous extract mediated synthesis of titanium dioxide nanoparticles. *Materials letter, 68,* 115-117.

Reza, K. M., Kurny, A., & Gulsham, F. (2017). Parameters affecting the photocatalytic degradation of dyes using TiO2: a review. *Applied Water Science, 7*, 1569–1578.

Roopan, S. A., Bharathi, A., Prabhakarn, A., AbdulRahuman, A., Velayuthan, K., Rajikumar, G., Madhumitha, G. (2012). Efficient phyto-synthesis and structural characterization of rutile TiO_2 nanoparticles using Annona squamosa peel extract. *Spectrochimica Acta Part A: Molecular and Biomolecular Spectroscopy , 98,* 86-90.

Saranya, K. S., Padil, V. V., Senan, C., Pilankatta, R., Saranya, K., George, B., Cˇerník, M. (2018). Green Synthesis of High Temperature Stable Anatase Titanium Dioxide Nanoparticles Using Gum Kondagogu: Characterization and Solar Driven Photocatalytic Degradation of Organic Dye. *Nanomaterials, 8*(1002), 1-19. doi:doi:10.3390/nano8121002

Shah, A. H., & Rather, M. A. (2021). Effect of calcination temperature on Crystallite size, particle size and Zeta potential of TiO2 Nanoparticles Synthesized via polyol-mediated method. *Materials Today, 44*, 482-488.

Singh, P., & Borthakur, A. (2018). A review on biodegradation and photocatalytic degradation of organic pollutants: A bibliometric and comparative analysis. *Journal of Cleaner Production, 196,* 1669-1680.

Srinivasan, M., Venkatesan, M., Arumugam, V., Natesan, G., Saravanan, N., Murugesan, S.,Pugazhendhi, A. (2019). Green synthesis and characterization of titanium dioxide nanoparticles (TiO2 NPs) using Sesbania grandiflora and evaluation of toxicity in zebrafish embryos. *Process Biochemistry, 80*, 197-202. doi:10.1016/j.procbio.2019.02.010

Subhapriya, S., & Gomathipriya, P. (2018). Green synthesis of titanium dioxide (TiO) nanoparticles by Trigonella foenum-graecum extract and its antimicrobial properties. *Microbial Pathogenesis, 116*, 215-220.

Sundrarajan, M., Bama, K., Bhavani, M., Jegatheeswaran, S., Ambika, S., Sangili, A., Sumathi, R. (2017). Obtaining titanium dioxide nanoparticles with spherical shape and antimicrobial properties using M. citrofolia leaves extract by hydrothermal method. *Journal of Phytochemistry and Photobiology, 171*, 117-124.

Suresh, P., Mehar, M. V., & Emmanuel, K. A. (2018). Factors Influencing the Rate of Photocatalytic Degradation of Hazardous Organic Pollutants fron Industrial Effluents: A Review. *International journal of Engineering Science Invention*, 18-22.

Umar, M., & Aziz, H. A. (2013). Photocatalytic Degradation of Organic Pollutants in Water. *Organic Pollutants - Monitoring, Risk and Treatment*, 195-208. doi:dx.doi.org/10.5772/53699

Velayutham, K., Rahuman, A. A., Rajakumar, G., Santhoshkumar, T., Marimuthu, S., & Jayaseelan, C. (2011). Evaluation of Catharanthus roseus leaf extract-mediated biosynthesis of titanium dioxide nanoparticles against Hippobosca maculata and Bovicola ovis. *Parasitol Resources, 111*(6), 2329-2337.

Vinoda, B. M., Vinuth, M., Yadav, D. B., & Manjana, J. (2015). Photocatalytic degradation of toxic methyl red dye using silica nanoparticles synthesized from rice husk ash. *Environmental and Analytical Technology, 5*(6), 1-5.

Yasmina, M., Mourad, K., Mohammed, S. H., & Khaoula, C. (2014). Treatment heterogenous photocatalysis; Factors influencing the photocatalytic degradation by TiO_2. *Energy Procedia, 50*, 559-566.

Ying, S., Guan, Z., Ofoegbu, P. C., Clubb, P., Rico, C., & Hong, J. (2022). Green synthesis of nanoparticles: Current developments and limitations. *Environmental Technology & Innovation, 26*, 102336.

Zeebaree, A. Y., Rashid, R. F., Zebari, O. I., Albarwry, A. J., Ali, A. F., & Zebari, A. Y. (2022). Sustainable engineering of plant-synthesized TiO_2 nanocatalysts: Diagnosis. properties and their photocatalytic performance in removing methylene blue dye from effluent. A review. *Current Research in Green and Sustainable Chemistry, 5*, 100312.

Zhu, S., & Wang, D. (2017). Photocatalysis: Basic Principles, Diverse Forms of Implementations and Emerging Scientific Opportunities. *Sdvanced Energy Materials*, 7, 1-24. doi:DOI: 10.1002/aenm.201700841